Article

Synthesis and Reactivity of Silyl Ruthenium Complexes: The Importance of Trans Effects in C–H Activation, Si–C Bond Formation, and Dehydrogenative Coupling of Silanes

Vladimir K. Dioumaev, Leo J. Procopio, Patrick J. Carroll, and Donald H. Berry

J. Am. Chem. Soc., **2003**, 125 (26), 8043-8058• DOI: 10.1021/ja035131p • Publication Date (Web): 10 June 2003

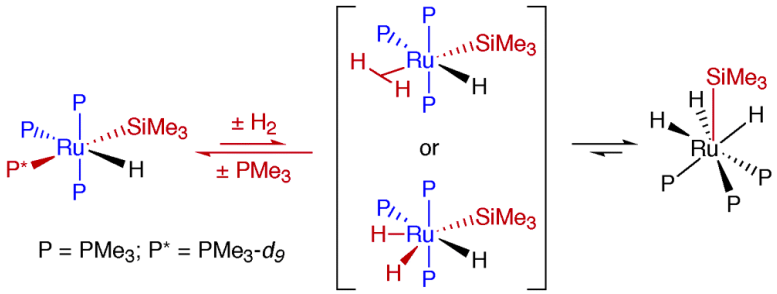

More About This Article

Additional resources and features associated with this article are available within the HTML version:

- Supporting Information
- Links to the 1 articles that cite this article, as of the time of this article download
- Access to high resolution figures
- Links to articles and content related to this article
- Copyright permission to reproduce figures and/or text from this article

View the Full Text HTML

J|A|C|S
ARTICLES
Published on Web 06/10/2003

Synthesis and Reactivity of Silyl Ruthenium Complexes: The Importance of Trans Effects in C−H Activation, Si−C Bond Formation, and Dehydrogenative Coupling of Silanes

Vladimir K. Dioumaev, Leo J. Procopio, Patrick J. Carroll, and Donald H. Berry*

Contribution from the Department of Chemistry and Laboratory for Research on the Structure of Matter, University of Pennsylvania, Philadelphia, Pennsylvania 19104-6323

Received March 13, 2003; E-mail: dberry@sas.upenn.edu

Abstract: A series of octahedral ruthenium silyl hydride complexes, *cis*-$(PMe_3)_4Ru(SiR_3)H$ (SiR_3 = $SiMe_3$, **1a**; $SiMe_2CH_2SiMe_3$, **1b**; $SiEt_3$, **1c**; $SiMe_2H$, **1d**), has been synthesized by the reaction of hydrosilanes with $(PMe_3)_3Ru(\eta^2\text{-}CH_2PMe_2)H$ (**5**), *cis*-$(PMe_3)_4RuMe_2$ (**6**), or $(PMe_3)_4RuH_2$ (**9**). Reaction with **6** proceeds via an intermediate product, *cis*-$(PMe_3)_4Ru(SiR_3)Me$ (SiR_3 = $SiMe_3$, **7a**; $SiMe_2CH_2SiMe_3$, **7b**). Alternatively, **1** and **7** have been synthesized via a fast hydrosilane exchange with another *cis*-$(PMe_3)_4Ru(SiR_3)H$ or *cis*-$(PMe_3)_4Ru(SiR_3)Me$, which occurs at a rate approaching the NMR time scale. Compounds **1a**, **1b**, **1d**, and **7a** adopt octahedral geometries in solution and the solid state with mutually cis silyl and hydride (or silyl and methyl) ligands. The longest Ru−P distance within a complex is always trans to Si, reflecting the strong trans influence of silicon. The aptitude of phosphine dissociation in these complexes has been probed in reactions of **1a**, **1c**, and **7a** with PMe_3-d_9 and CO. The dissociation is regioselective in the position trans to a silyl ligand (trans effect of Si), and the rate approaches the NMR time scale. A slower secondary process introduces PMe_3-d_9 and CO in the other octahedral positions, most likely via nondissociative isomerization. The trans effect and trans influence in **7a** are so strong that an equilibrium concentration of dissociated phosphine is detectable (~5%) in solution of pure **7a**. Compounds **1a**−**c** also react with dihydrogen via regioselective dissociation of phosphine from the site trans to Si, but the final product, *fac*-$(PMe_3)_3Ru(SiR_3)H_3$ (SiR_3 = $SiMe_3$, **4a**; $SiMe_2CH_2SiMe_3$, **4b**; $SiEt_3$, **4c**), features hydrides cis to Si. Alternatively, **4a**−**c** have been synthesized by photolysis of $(PMe_3)_4RuH_2$ in the presence of a hydrosilane or by exchange of *fac*-$(PMe_3)_3Ru(SiR_3)H_3$ with another $HSiR_3$. The reverse manifold − HH elimination from **4a** and trapping with PMe_3 or PMe_3-d_9 − is also regioselective (**1a-d_9** is predominantly produced with PMe_3-d_9 trans to Si), but is very unfavorable. At 70 °C, a slower but irreversible SiH elimination also occurs and furnishes $(PMe_3)_4RuH_2$. The structure of **4a** exhibits a tetrahedral P_3Si environment around the metal with the three hydrides adjacent to silicon and capping the P_2Si faces. Although strong Si···HRu interactions are not indicated in the structure or by IR, the HSi distances (2.13−2.23(5) Å) suggest some degree of nonclassical SiH bonding in the H_3SiR_3 fragment. Thermolysis of **1a** in C_6D_6 at 45−55 °C leads to an intermolecular CD activation of C_6D_6. Extensive H/D exchange into the hydride, $SiMe_3$, and PMe_3 ligands is observed, followed by much slower formation of *cis*-$(PMe_3)_4Ru(D)(Ph\text{-}d_5)$. In an even slower intramolecular CH activation process, $(PMe_3)_3Ru(\eta^2\text{-}CH_2PMe_2)H$ (**5**) is also produced. The structure of intermediates, mechanisms, and aptitudes for PMe_3 dissociation and addition/elimination of H−H, Si−H, C−Si, and C−H bonds in these systems are discussed with a special emphasis on the trans effect and trans influence of silicon and ramifications for SiC coupling catalysis.

Introduction

Catalytic formation of SiC bonds from CH- and SiH-containing substrates are rare examples of efficient catalytic CH bond functionalization.[1−4] The side product of these reactions is either dihydrogen (coupling of hydrosilanes with aromatic substrates and dehydrogenative coupling of alkylsilanes to carbosilanes) or alkane (transfer dehydrogenative coupling with a sacrificial olefin). Many of these reactions were reported for $18e^-$ complexes of ruthenium, $(PMe_3)_4Ru(SiR_3)H$ (**1**) or $(PMe_3)_3Ru(SiR_3)H_3$ (**4**). It has been long recognized that the true catalytic species in these processes are $16e^-$ $(PMe_3)_3Ru(SiR_3)R$ and $18e^-$ $(PMe_3)_3Ru(SiR_3)_a(R)_bH_c$ ($a + b + c = 4$, R = H, alkyl, or aryl), which interconvert via addition/elimination of HH, SiH, CH, and SiC bonds. The aptitude and selectivity for the addition of SiH and CH bonds versus elimination of SiC and HH (or another CH) directly impact the rate of the dehydrogenative (or dealkanative) catalysis. These issues are particularly acute in the case of $(PMe_3)_3Ru(SiR_3)_a(R)_bH_c$ intermediates, which can conceivably eliminate any combination of HH, CH, SiH, SiC,

(1) Procopio, L. J.; Berry, D. H. *J. Am. Chem. Soc.* **1991**, *113*, 4039−4040.
(2) Procopio, L. J.; Mayer, B.; Plössl, K.; Berry, D. H. *Polym. Prepr. (Am. Chem. Soc., Div. Polym. Chem.)* **1992**, *33*, 1241−1242.
(3) Djurovich, P. I.; Dolich, A. R.; Berry, D. H. *J. Chem. Soc., Chem. Commun.* **1994**, 1897−1898.
(4) Ezbiansky, K.; Djurovich, P. I.; LaForest, M.; Sinning, D. J.; Zayes, R.; Berry, D. H. *Organometallics* **1998**, *17*, 1455−1457.

10.1021/ja035131p CCC: $25.00

CC, or SiSi bonds. Indeed, each of the above elimination processes has been separately observed, and there are precedents for competitive eliminations in $M(SiR_3)(R)H$ species.[5−10]

The aptitude for addition/elimination is readily understood in terms of bond disruption enthalpies (BDE) and the size and directionality of the orbitals involved. The usual order − HH ≈ SiH (fast) > CH > SiC (slow) − is not particularly favorable for the CSi bond formation catalysis; however, interesting exceptions exist. For example, an unusual acceleration has been reported for hydrosilylation reactions with chelating hydrosilanes.[11−13] The effect correlates with the length of chelating linkage, and the best rates are achieved with a 2−3 carbon atom bridge. The catalytic species have been studied by NMR and concluded to be bis(silyl) trihydrides, $(PPh_3)_2Rh(R_2Si{\sim}SiR_2)(H)_3$.[13] In contrast, only monosilyl species were detected with nonchelating silanes under identical conditions.[13] It has been suggested that the presence of the second silyl on the metal and the geometrical restrictions imposed by the chelate facilitate addition/elimination processes.

The ability of silicon to labilize other ligands, especially those trans to Si, has been noted previously.[14] Particularly relevant for this paper are examples of the trans effect in six-[15−18] and seven-coordinate complexes.[19,20] In addition to the kinetic consequences, silyl ligands are also known for a ground-state phenomenon of weakening and elongation of the metal ligand bonds trans to silicon. This thermodynamic trans influence has been used to explain bond elongation in the structures of six-[7,8,18,19,21−27] and seven-coordinate complexes[20] as well as the stability of five-coordinate 16e$^-$ species with an empty site trans to Si.[28−30] Because silyl species are inherently present in all catalytic SiC coupling processes, it is of interest to study the role of the silicon trans effects and influences on the chemistry of ruthenium silyl compounds and exploit this information to design optimal catalysts.

We now report the synthesis of a series of silyl ruthenium complexes, precursors to SiC coupling catalysts. Dissociation of PMe_3 and addition/elimination of H−H, Si−H, C−Si, and C−H bonds in these systems are studied with a special emphasis on the trans effect/influence of silicon and are discussed in the context of SiC coupling catalysis.

Results

Synthesis and Characterization of *cis*-$(PMe_3)_4Ru(SiR_3)H$ Complexes. Ruthenium silyl hydride complexes *cis*-$(PMe_3)_4Ru(SiR_3)H$ (**1**) have been prepared by three main methods. Our original synthesis involved photolysis of $(PMe_3)_3Ru(\eta^2\text{-}CH_2PMe_2)H$, **5**,[31,32] in the presence of excess trimethylsilane leading to isolation of *cis*-$(PMe_3)_4Ru(SiMe_3)H$ (**1a**, eq 1) in 59% yield. The triethylsilyl derivative *cis*-$(PMe_3)_4Ru(SiEt_3)H$ (**1c**) was prepared similarly from $HSiEt_3$ in 37% yield. *cis*-$(PMe_3)_4Ru(SiMe_2H)H$ (**1d**) was prepared in 80% yield by photolysis of a different precursor, $(PMe_3)_4RuH_2$ (**9**), in excess H_2SiMe_2. Note that this approach depends on the unfavorable equilibrium between the initially formed $(PMe_3)_3Ru(H)_3(SiMe_2H)$ with **1d** (vide infra) and is not a viable synthetic reaction for larger silyl groups.

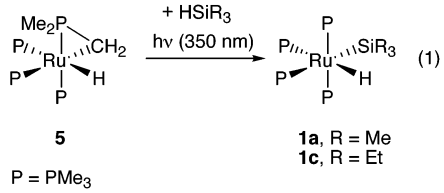

5 P = PMe_3 **1a**, R = Me **1c**, R = Et

However, these methods require rather long reaction times (ca. 10 days), and it was subsequently found that silyls can be more conveniently prepared by the reaction of $(PMe_3)_4RuMe_2$ (**6**) and excess hydridosilane at 60 °C (eq 2). The major byproducts of this reaction are CH_4, $MeSiR_3$, and a carbosilane produced by dehydrocoupling of the starting silane. In many cases, these materials are volatile and easily separated from the ruthenium silyl product. Prolonged reaction times at higher temperatures result in further dehydrocoupling to less volatile silane products and contamination of the products with trihydride complexes, **4**, both of which complicate isolation of the silyl hydrides, **1**.

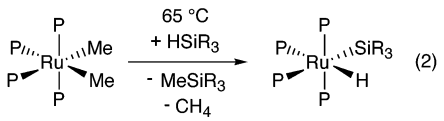

6 P = PMe_3 **1a**, SiR_3 = $SiMe_3$ **1b**, SiR_3 = $SiMe_2CH_2SiMe_3$

In many instances, the most convenient route to analogous ruthenium silyl complexes is the equilibrium exchange of the rather hindered and labile *cis*-$(PMe_3)_4Ru(SiMe_3)H$ (**1a**) with other hydridosilanes (eq 3). The reaction is rapid at room temperature, and the volatility of $HSiMe_3$ facilitates its removal.

(5) Thorn, D. L.; Harlow, R. L. *Inorg. Chem.* **1990**, *29*, 2017−2019.
(6) Cleary, B. P.; Mehta, R.; Eisenberg, R. *Organometallics* **1995**, *14*, 2297−2305.
(7) Aizenberg, M.; Milstein, D. *Angew. Chem.* **1994**, *106*, 344−346 (See also: *Angew. Chem., Int. Ed. Engl.* **1994**, *19*33, 1317−1319).
(8) Aizenberg, M.; Milstein, D. *J. Am. Chem. Soc.* **1995**, *117*, 6456−6464.
(9) Mitchell, G. P.; Tilley, T. D. *Organometallics* **1998**, *17*, 2912−2916.
(10) Goikhman, R.; Aizenberg, M.; Ben-David, Y.; Shimon, L. J. W.; Milstein, D. *Organometallics* **2002**, *21*, 5060−5065.
(11) Nagashima, H.; Tatebe, K.; Itoh, K. *J. Chem. Soc., Perkin Trans. 1* **1989**, 1707−1708.
(12) Nagashima, H.; Tatebe, K.; Ishibashi, T.; Sakakibara, J.; Itoh, K. *Organometallics* **1989**, *8*, 2495−2496.
(13) Nagashima, H.; Tatebe, K.; Ishibashi, T.; Nakaoka, A.; Sakakibara, J.; Itoh, K. *Organometallics* **1995**, *14*, 2868−2879.
(14) Chatt, J.; Eaborn, C.; Ibekwe, S. D.; Kapoor, P. N. *J. Chem. Soc. A* **1970**, 1343.
(15) (a) Pomeroy, R. K.; Gay, R. S.; Evans, G. O.; Graham, W. A. G. *J. Am. Chem. Soc.* **1972**, *94*, 272−274. (b) Pomeroy, R. K. *J. Organomet. Chem.* **1979**, *177*, C27.
(16) Pomeroy, R. K.; Wijesekera, K. S. *Inorg. Chem.* **1980**, *19*, 3729−3735.
(17) Pomeroy, R. K.; Hu, X. *Can. J. Chem.* **1982**, *60*, 1279−1285.
(18) Haszeldine, R. N.; Parish, R. V.; Setchfield, J. H. *J. Organomet. Chem.* **1973**, *57*, 279−285.
(19) Okazaki, M.; Ohshitanai, S.; Iwata, M.; Tobita, H.; Ogino, H. *Coord. Chem. Rev.* **2002**, *226*, 167−178.
(20) Dioumaev, V. K.; Yoo, B. R.; Procopio, L. J.; Carroll, P. J.; Berry, D. H. *J. Am. Chem. Soc.*, in press.
(21) Crozat, M. M.; Watkins, S. F. *J. Chem. Soc., Dalton Trans.* **1972**, 2512.
(22) Holmes-Smith, R. D.; Stobart, S. R.; Vefghi, R.; Zaworotko, M. J.; Jochem, K.; Cameron, T. S. *J. Chem. Soc., Dalton Trans.* **1987**, 969.
(23) Zlota, A. A.; Frolow, F.; Milstein, D. *J. Chem. Soc., Chem. Commun.* **1989**, 1826−1827.
(24) Levy, C. J.; Puddephatt, R. J.; Vittal, J. J. *Organometallics* **1994**, *13*, 1559−1560.
(25) Levy, C. J.; Vittal, J. J.; Puddephatt, R. J. *Organometallics* **1996**, *15*, 2108−2117.
(26) Coe, B. J.; Glenwright, S. J. *Coord. Chem. Rev.* **2000**, *203*, 5−80.
(27) Reinartz, S.; White, P. S.; Brookhart, M.; Templeton, J. L. *Organometallics* **2000**, *19*, 3748−3750.
(28) Heyn, R. H.; Macgregor, S. A.; Nadasdi, T. T.; Ogasawara, M.; Eisenstein, O.; Caulton, K. G. *Inorg. Chim. Acta* **1997**, *259*, 5−26.
(29) Dioumaev, V. K.; Plössl, K.; Carroll, P. J.; Berry, D. H. *J. Am. Chem. Soc.* **1999**, *121*, 8391−8392.
(30) Dioumaev, V. K.; Ploessl, K.; Carroll, P. J.; Berry, D. H. *Organometallics* **2000**, *19*, 3374−3378.
(31) Werner, H.; Werner, R. *J. Organomet. Chem.* **1981**, *209*, C60.
(32) Gotzig, J.; Werner, R.; Werner, H. *J. Organomet. Chem.* **1985**, *290*, 99.

The equilibrium substitution with a silyl group smaller than $SiMe_3$ (e.g., $SiMe_2H$**)** is quite facile, whereas exchange with larger silyls such as $SiMe_2CH_2SiMe_3$ is not favored ($K_{eq}(300) \approx 6.5 \times 10^{-3}$) and requires excess silane and periodic removal of $HSiMe_3$ during the reaction. At temperatures below ~60 °C, no decomposition or polymerization products are produced, and workup is straightforward. In the case of low boiling silanes, removal of all volatiles under vacuum yields the pure ruthenium silyl product quantitatively. The rate of exchange with **1a** with free silane approaches the NMR time scale (500 MHz, 30 °C), as is evident from the drift of the $RuSiMe_3$ ^{1}H NMR resonance ($\Delta\delta = 0.10$) in the presence of ca. 10 equiv of $HSiMe_3$. Degenerate exchange is chemically verified by the rapid incorporation of deuterium in the hydride position of **1a** in reactions with $DSiMe_3$.

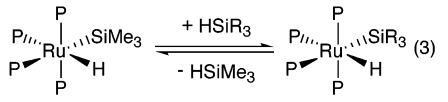

1a **1b**, $SiR_3 = SiMe_2CH_2SiMe_3$

P = PMe_3

The *cis*-octahedral structures of the silyl hydride complexes are clearly established by three distinct phosphine environments in a 2:1:1 ratio in ^{1}H and ^{31}P NMR spectra and strong virtual coupling between mutually trans phosphines in the ^{1}H NMR spectra. The hydride and silyl ligands are readily identified by characteristic chemical shifts and multiplicities: ^{1}H NMR ca. δ −11 (dtd or dq) for Ru*H* and ca. δ 0.7−1.0 for RuSi*Me*$_n$. The silyl resonances are found between δ 11 and −1 ppm in the ^{29}Si NMR. The classical nature of the hydride and silyl ligands is strongly suggested by the ruthenium−hydride stretching frequencies in the IR spectrum (ν(RuH) = ca. 1820−1790 cm^{-1}); significant agostic Si···H interactions would decrease this value below ca. 1650 cm^{-1}.[20] Further confirmation of the classical nature of the silyl hydride complexes is found in the solid-state structures, vide infra.

Products and Processes in the Reaction of $HSiMe_3$ with 6. The reaction of **6** with $HSiMe_3$ at 60 °C is a very convenient synthetic route to **1a**, but the stoichiometry of the reaction suggests a fairly complicated mechanism involving competitive C−H and C−Si elimination pathways which warranted closer scrutiny. The thermal reaction of **6** with ca. 10 equiv of $HSiMe_3$ (18 h, 60 °C) yields **1a** (1 equiv), $SiMe_4$ (0.25 equiv), $HSiMe_2CH_2SiMe_3$ (0.75 equiv), and CH_4 (not quantified.) No other ruthenium complexes are observed, except for traces of **1b**, which is in equilibrium with **1a**.

However, treatment of **6** with $HSiMe_3$ at room temperature permits observation of an intermediate complex, *cis*-$(PMe_3)_4Ru(SiMe_3)Me$ (**7a**). For example, after 18 h, the reaction mixture consists of 40% **6**, 50% **7a**, and ~10% silyl hydride species **1a** and **1b**. Further reaction leads to a decrease in the concentration of **7a**, and increased amounts of **1a** and **1b**, which are in equilibrium with each other and the respective hydridosilanes (eq 4). A pure sample of **7a** was isolated from **1a**, **1b**, and **6** with some difficulty via fractional crystallization (ca. 13% yield). The spectral features of the silyl and phosphine ligands in **7a** are similar to those of **1a**, **1b**, or **1c**, and a multiplet at δ −0.68 in the ^{1}H NMR can be assigned to the methyl group on ruthenium. However, rapid phosphine dissociation on the NMR time scale obscures much of the scalar coupling in the ^{1}H and ^{31}P NMR spectra, and the structural assignment is most reliably confirmed by the single-crystal X-ray diffraction study (vide infra). In a separate experiment, treatment of **7a** with a large excess of $HSiMe_2CH_2SiMe_3$ leads to equilibrium amounts of $(PMe_3)_4Ru(SiMe_2CH_2SiMe_3)Me$, **7b** ($K_{eq}(300) = 5.9 \times 10^{-3}$). Compound **7b** was not isolated and was identified by ^{1}H NMR spectroscopy. As in the case of **1a**, **7a** undergoes rapid exchange with free silane as indicated by a shift of the $RuSiMe_3$ ^{1}H NMR resonance in the presence of $HSiMe_3$.

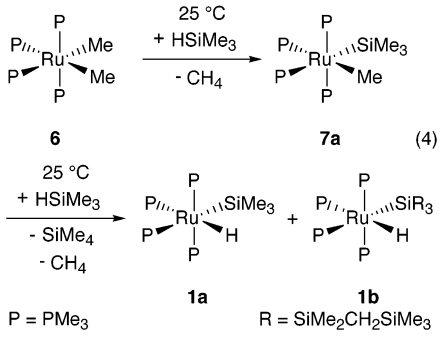

6 **7a** **1a** **1b**

P = PMe_3 R = $SiMe_2CH_2SiMe_3$

Phosphine Lability in $(PMe_3)_4Ru(SiR_3)X$ Complexes: Reactions with PMe_3-d_9. Many of the silyl complexes described above exhibit much greater phosphine lability than is found in other known *cis*-$(PMe_3)_4Ru(X)(Y)$ complexes (X, Y = H, Me, Cl). For example, treatment of **1a** with excess PMe_3-d_9 at 25 °C is fast (<5 min) and highly regioselective: 1 equiv of unlabeled phosphine is released, and the labeled ligand is incorporated into only one position in the complex (eq 5). The ^{31}P NMR resonance for the exchanged phosphine site shifts by ca. 2.4 ppm upfield from δ −17 in **1a** to −19.4 in **1a-*d*$_9$**, whereas the other resonances are unperturbed. Significantly, this same phosphine resonance shows slight broadening in the presence of free PMe_3, suggesting the rate of the exchange process is approaching the NMR time scale (25 °C, 80 MHz). For comparison, phosphine dissociation from the dihydride, P_4RuH_2 (**9**), requires hours at 120 °C.

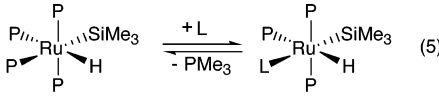

1a **1a-*d*$_9$**, L = $P(CD_3)_3$

P = PMe_3

The specific site of PMe_3 exchange in **1a** can be assigned to that trans to the silyl ligand by selective $\{^1H\}^{31}P$ experiments: decoupling only the methyl groups of **1a** reveals strong coupling between only one phosphine and the ruthenium hydride (δ −15.2, $J_{PH} \approx 61$ Hz). This resonance is thus due to the phosphine trans to the hydride. As the equivalent, mutually trans, phosphines can be conclusively assigned on the basis of the normal $\{^1H\}^{31}P$ spectrum, the remaining resonance (δ −17) − the extremely labile position − can be, therefore, attributed to the PMe_3 ligand trans to the trimethylsilyl group. Although the initial phosphine exchange is site selective, reaction of **1a** with PMe_3-d_9 eventually leads to incorporation of labeled phosphine into all of the sites. However, the process is fairly slow, and a statistical distribution is reached only after weeks at 25 °C in the presence of ca. 12 equiv of PMe_3-d_9. Reactions of the more

sterically crowded **1c** with PMe_3-d_9 are also initially selective, but secondary scrambling is faster than in **1a**. Thus, selective incorporation of labeled phosphine into the position trans to the silyl in **1c** also occurs in <5 min, but scrambling into all sites is complete in <1 h (^{1}H NMR).

Selective exchange with PMe_3-d_9 with the methyl silyl complex **7a** occurs rapidly on the NMR time scale at room temperature. The phosphine presumed trans to silicon (in the absence of exchange: ^{1}H NMR δ 0.98, ^{31}P NMR δ −21.7) is in coalescence with free PMe_3 (^{1}H NMR δ 0.78, ^{31}P NMR δ −62.5) or with PMe_3-d_9 (^{31}P NMR δ −65.5), and coupling to the other phosphines in **7a** is lost. In this case, further exchange of labeled ligand into the other positions occurs within minutes (ca. 20% in 3 min). In contrast, **5**, which does not bear silyl ligands, is considerably less prone to phosphine dissociation and exchange (ca. 50% exchange after 102 h at 65 °C or ca. 20% exchange after 24 h of photolysis at 350 nm).

Furthermore, the equilibrium concentration of the 16e$^-$ species generated from **7a** (eq 6) is sufficiently high to be detected. At 300 K, an isolated sample of **7a** exhibits a very broad ^{31}P NMR resonance at δ −22.80 ($\nu_{1/2}$ = 700 Hz), and no free PMe_3 is detected. However, at 240 K, two signals decoalesce: δ −20.28 for the phosphine trans to Si in **7a** and −62.5 corresponding to ca. 7% free PMe_3. The amount of free PMe_3 decreases to <5% at 190 K. Discrete ^{31}P signals for **7a** and the 16e$^-$ $(PMe_3)_3Ru(SiMe_3)Me$ are not resolved, presumably due to much smaller frequency differences of the coordinated phosphines in these exchanging species as compared to $\Delta\delta \approx$ 42 ppm for coordinated and free ligand. Additional evidence for appreciable concentrations of the unsaturated ruthenium complex is found in the dependence of the Si*Me*$_3$ chemical shift for **7a** on temperature (e.g., ^{1}H NMR (C_7D_8): δ 0.49 at 300 K vs δ 0.81 at 190 K), and upon phosphine concentration (δ (C_6D_{12}, 338 K) δ 0.12 without phosphine and δ 0.15 in the presence of 5 equiv of added PMe_3).

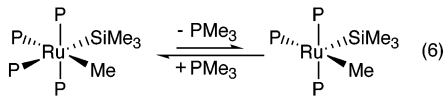

(6)

7a P = PMe_3

The 18e$^-$/16e$^-$ equilibrium also explains the coloration of **7a** in solution. Saturated ruthenium(II) complexes such as **1a** and **6** are colorless as solids and in solution at room temperature, whereas isolated 16e$^-$ $(PMe_3)_3Ru(SiMe_3)H$, **2a**, is brown-red.[29,30] However, solutions of the ostensibly 18e$^-$ **7a** are red-brown at room temperature and bleach to colorless in the presence of 5 equiv of PMe_3. Unfortunately, attempts to isolate 16e$^-$ $(PMe_3)_3Ru(SiMe_3)Me$ employing BPh_3 and other phosphine sponges as described previously for **1a**[29,30] were not successful and led to a plethora of decomposition products.

Reactions with CO and Synthesis of $(CO)(PMe_3)_3Ru(SiMe_3)H$. Given the phosphine exchange reactions described above, it is not surprising that **1a** reacts rapidly with carbon monoxide to yield 1 equiv of free PMe_3 and *mer*-$(CO)(PMe_3)_3Ru(SiMe_3)H$ (***mer*-8**), the monocarbonyl with CO trans to silicon (eq 7). The reaction is quantitative by ^{1}H NMR, but isolation of ***mer*-8** was thwarted by rapid isomerization at room temperature to the facial isomer, *fac*-$(CO)(PMe_3)_3Ru(SiMe_3)H$ (***fac*-8**, eq 7).

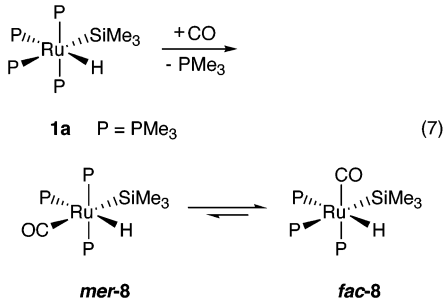

At room temperature, a benzene-d_6 solution of ***mer*-8** converts to ***fac*-8** with a half-life of ca. 35 min, ultimately yielding an equilibrium ratio of 95% ***fac*-8** to 5% ***mer*-8**, and recrystallized product redissolves to yield the same 95:5 mixture. The *mer*/*fac* isomerization appears to be nondissociative, as isomerization of ***mer*-8** proceeds in the presence of free PMe_3-d_9 or excess CO to initially yield only ***fac*-8-d_0**, that is, without incorporation of labeled phosphine or a second CO on the time scale of isomerization.

The unstable ***mer*-8** exhibits two distinct phosphine environments in a 2:1 ratio that are characteristic of a cis,cis,trans (*mer*) arrangement (^{1}H NMR δ 1.29 (t) and 1.10 (d); ^{31}P NMR δ −7.0 (d) and 15.7 (t)). The larger coupling of the Ru−H resonance (δ −9.07, dt, J_{PH} = 73.8 and 29.1 Hz) establishes the mutually trans relationship between the hydride and a phosphine and, therefore, mutually trans position of CO and Si ligands. The other isomer, ***fac*-8**, exhibits three phosphine environments (^{1}H NMR δ 1.123, 1.117, and 1.09; ^{31}P NMR δ −11.2, −15.9, and −22.0) consistent with the facial geometry. The multiplicity of the NMR resonances of the hydride (^{1}H NMR: ddd, J_{PH} = 67.1, 29.9, and 21.4 Hz), carbonyl (^{13}C NMR: dt, J_{PC} = 79.3 and 9.0 Hz), and the silyl (^{29}Si NMR: ddd, J_{PSi} = 74.8, 21.0, 11.3 Hz) ligands confirms facial geometry − each nonphosphine ligand exhibits a single large scalar coupling constant due to a trans phosphine. The IR spectrum exhibits strong bands for classical RuH and terminal carbonyl ligands (ν(CO) = 1932 cm^{-1}; ν(RuH) = 1858 cm^{-1}).

Reactions with Dihydrogen and Synthesis of $(PMe_3)_3Ru(SiR_3)H_3$ Complexes. The ease of phosphine dissociation from $(PMe_3)_4Ru(SiR_3)H$ complexes also manifests itself in rapid reactions with dihydrogen under mild conditions. Thus, **1a** and **1c** react with dihydrogen to produce free PMe_3 and $(PMe_3)_3Ru(SiMe_3)H_3$ (**4a**) or $(PMe_3)_3Ru(SiEt_3)H_3$ (**4c**) in quantitative yield in <5 min at room temperature (eq 8). It is noteworthy that reaction of **1a-d_9** (labeled phosphine trans to silicon) with hydrogen leads to formation of only **4a-d_0** and free PMe_3-d_9 as determined by ^{1}H NMR. This regiospecificity strongly suggests the reaction proceeds via the same intermediate as does the phosphine exchange process.

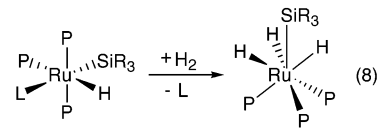

(8)

1a, R = Me, L = PMe_3
1a-d_9, R = Me, L = PMe_3-d_9
1c, R = Et, L = PMe_3

4a, R = Me
4c, R = Et

P = PMe_3

In contrast, the dimethylsilyl derivative, **1d**, is apparently more stable than the corresponding trihydride complex, which

could not be isolated. Treatment of **1d** with 3 atm H_2 in an NMR tube generated only ca. 10% free PMe_3. A new hydride resonance at δ −9.7 was also observed, but reversion to **1d** occurred upon removal of hydrogen pressure.

A more general method for the synthesis of the Ru(IV) trihydride silyls (**4a**−**c**) is the photolytic reaction (350 nm) of an appropriate hydridosilane with the more readily available *cis*-$(PMe_3)_4RuH_2$, **9** (eq 9).[1,33] Alternatively, **4b**, **4c**, and other derivatives can be conveniently prepared in quantitative yield by exchange of **4a** with an excess of the appropriate hydridosilane $HSiR_3'$ at room temperature. As in the case of silyl exchange with **1a**, this equilibrium is sensitive to the relative steric demands of the silyl ligands, but use of excess $HSiR_3'$ and removal of $HSiMe_3$ permits quantitative conversion in the cases examined. For example, the reaction of **4a** with $HSiMe_2CH_2SiMe_3$ is complete in minutes, generating **4b** and $HSiMe_3$.[20]

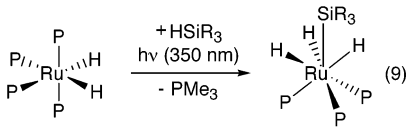

9 P = PMe_3

4a, SiR_3 = $SiMe_3$
4b, SiR_3 = $SiMe_2CH_2SiMe_3$
4c, SiR_3 = $SiEt_3$

The same equilibrium mixture is obtained by reaction of **4b** with $HSiMe_3$. The reaction clearly favors the smaller silyl ligand bound to ruthenium ($K_{eq}(298) = 1.2 \times 10^{-2}$). The exchange of the bulkier $HSiEt_3$ (ca. 1 equiv) with **4a** is very slow and yields a 4:1 mixture of **4a**:**4c** after 2 weeks at room temperature. Interestingly, the complementary reaction − the bulky silyl trihydride **4c** with 1 equiv of $HSiMe_3$ at 25 °C − is also extremely slow. The less hindered **4a** was not detected after 2 days (<2%), and the equilibrium ratio was not achieved after 2 weeks (**4a**:**4c** = 1:4).

The ruthenium hydride resonances in **4a**−**c** in the ^1H NMR appear as a complicated pattern with two sharp peaks centered within a broad multiplet at ca. δ −10. Although the line shape may suggest a dynamic process, complexes **4a** and **4b** are not fluxional on the NMR time scale and show only a slight broadening of the RuH resonances as the temperature is lowered to 190 K. The line shape is in fact due to the three-fold symmetry of the *fac*-RuH_3P_3 fragment and resultant AA′A″XX′X″ spin system. Overall, the NMR features closely resemble those of previously described $L_3M(ER_3)H_3$ complexes.[20,34−41] The spectroscopic assignment was confirmed by single-crystal X-ray diffraction analysis of **4a**, vide infra, and **4b**.[20] The absence of appreciable nonclassical H···H interactions is suggested by the IR spectra (Nujol: ν(RuH) = 1890 cm^{-1} for **4a** and 1899 cm^{-1} for **4c**), and relaxation constants (200 MHz, C_6D_6, 25 °C, T_1 = 1500 ms for **4a** and 1025 ms for **4c**), and has been confirmed by a neutron diffraction study on **4a**.[42]

Reactions of $(PMe_3)_3Ru(SiR_3)H_3$ with PMe_3-d_9 and D_2. In contrast to the rapid, regiospecific incorporation of labeled phosphine into octahedral silyl complexes such as **7a** and **1a**, no exchange was detected in the reaction of **4a** with 12 equiv of PMe_3-d_9 after 30 days at 25 °C. Incorporation of PMe_3-d_9 was observed following photolysis of **4a** (350 nm, 10 °C.)

Although **4a** does not undergo net exchange with labeled phosphine, hydrogen dissociation does occur at room temperature, but the equilibrium strongly favors the seven-coordinate trihydride complex. Thus, treatment of **4a** in neat PMe_3 for 20 h at room temperature and removal of all volatiles (including hydrogen) yields a mixture containing mainly unreacted **4a** (80%) and 20% of the tetrakis phosphine complex **1a** (eq 10). Furthermore, introduction of H_2 onto neat PMe_3 solutions of **1a** generates **4a** quantitatively very rapidly at room temperature.

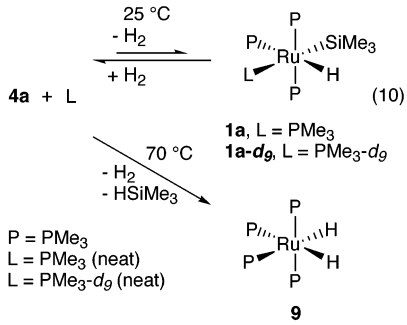

Repeating this experiment in neat PMe_3-d_9 reveals that the preponderance of labeled phosphine in **1a** is found trans to the $SiMe_3$ group; <20% label is observed in the other three sites combined after 20 h in neat PMe_3-d_9. Recall that slow secondary scrambling of labeled phosphine was found in the studies of **1a** described above.

The ease of H_2 elimination from **4a** is clearly illustrated by the reaction with D_2, where the rate is not masked by an unfavorable equilibrium. Treatment of **4a** with ca. 3 atm D_2 at room temperature for <5 min yields H_2 and **4a**-d_2 and <5% HD, consistent with a mechanism requiring the initial reductive elimination of H_2. Naturally, HD is observed after longer reaction times, produced by subsequent elimination from **4a**-d_2. Compound **4b** also exchanges Ru−H positions with D_2 rapidly at room temperature, but H/D exchange occurs only very slowly with the triethylsilyl complex, **4c**. Only trace amounts of H_2 and HD are detected by ^1H NMR after days at 25 °C.

Another possible reaction of **4a** − Me_3SiH elimination − is extremely slow. Reactions of **4a** in neat PMe_3 at room temperature do not yield detectable quantities of the *cis*-dihydride complex (**9**). However, thermolysis of **4a** at 70 °C in the presence of ∼2 equiv of PMe_3 results in the slow, but quantitative, conversion to **9** (115 h, eq 10). Compound **9** is virtually inert toward reactions with Me_3SiH or phosphine exchange below ca. 100 °C. Thus, Si−H elimination from **4a** cannot be occurring to a significant extent at 25 °C, even though H−H elimination is rapid.

CH Activation and SiH Elimination in the $(PMe_3)_4Ru(SiR_3)H$ Complexes. Another important aspect of the chemistry of these silyl ruthenium complexes is the ability to activate CH

(33) Montiel-Palma, V.; Perutz, R. N.; George, M. W.; Jina, O. S.; Sabo-Etienne, S. *Chem. Commun.* **2000**, 1175−1176.
(34) Gilbert, S.; Knorr, M.; Mock, S.; Schubert, U. *J. Organomet. Chem.* **1994**, *480*, 241−254.
(35) Hubler, K.; Hubler, U.; Roper, W. R.; Schwerdtfeger, P.; Wright, L. J. *Chem.-Eur. J.* **1997**, *3*, 1608−1616.
(36) Knorr, M.; Gilbert, S.; Schubert, U. *J. Organomet. Chem.* **1988**, *347*, C17−C20.
(37) Mohlen, M.; Rickard, C. E. F.; Roper, W. R.; Salter, D. M.; Wright, L. J. *J. Organomet. Chem.* **2000**, *593*−*594*, 458−464.
(38) Rickard, C. E. F.; Roper, W. R.; Woodgate, S. D.; Wright, L. J. *J. Organomet. Chem.* **2000**, *609*, 177−183.
(39) Schubert, U.; Gilbert, S.; Mock, S. *Chem. Ber.* **1992**, *125*, 835−837.
(40) Burn, M. J.; Bergman, R. G. *J. Organomet. Chem.* **1994**, *472*, 43−54.
(41) Feldman, J. D.; Peters, J. C.; Tilley, T. D. *Organometallics* **2002**, *21*, 4065−4075.
(42) Koetzle, T.; Wu, P., unpublished results.

bonds. Activation of aryl CH bonds by ruthenium(0) complexes is not that unusual, but CH bond addition to a 16e$^-$ ruthenium(II) species such as $(PMe_3)_3Ru(SiR_3)H$ is of particular interest as the resultant species can potentially undergo elimination of CH-, SiC-, SiH-, or HH-bonds. The course of these elimination reactions has a direct bearing on catalytic processes such as functionalization of CH bonds, hydrosilylation, dehydrogenative coupling, and transfer dehydrogenative coupling of silanes to oligocarbosilanes, and, therefore, deserves closer scrutiny.

Thermolysis of **1a** in benzene at 65 °C leads to CH bond activation of the solvent and formation of *cis*-$(PMe_3)_4Ru(H)(Ph)$, **10** (eq 11). The trimethylsilane formed must be removed periodically to drive the equilibrium and to avoid subsequent dehydrocoupling to carbosilane ($HSiMe_2CH_2SiMe_3$) and dihydrogen, both of which lead to additional ruthenium products. The phenyl derivative **10** was isolated in 79% yield after ~14 days at 65 °C, and the spectroscopic parameters match those reported by Bergman and co-workers.[43]

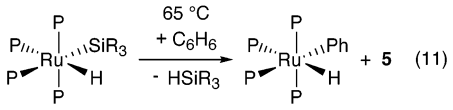

1a, $SiR_3 = SiMe_3$
1c, $SiR_3 = SiEt_3$ P = PMe_3 **10**

Thermolysis of **1a** in C_6D_6 at 45 °C for 15 h leads to extensive H/D exchange between C_6D_6 and **1a**, and only trace amounts of deuterated **10**. Approximately 18% deuteration of the $SiMe_3$ group and 8% of the PMe_3 ligands was observed. After 16 h at 55 °C, <10% **10** was produced, but the ^{1}H NMR signal for the $SiMe_3$ ligand of **1a** had decreased by 80%, and those for the PMe_3 ligands had decreased by 40%. Corresponding increases in intensity were observed in the ^{2}H NMR spectra. In a slower process, **5** (~10% after 90 h at 55 °C) is also produced by intramolecular CH activation. Addition of free PMe_3 (3 equiv) completely inhibits both the H/D exchange and the formation of **10**, but does not affect production of **5** (~8% in 90 h at 55 °C). Compound **5** is the only new ruthenium product observed when thermolysis of **1a** is performed in cyclohexane-d_{12}, and no H/D scrambling is observed, consistent with a clear preference for an intramolecular activation of a primary CH bond over intermolecular activation of the secondary aliphatic CD. Thermolysis of the triethylsilyl complex **1c** in benzene also produces the phenyl complex **10**, but the reaction is 2−3× faster than that for the less hindered **1a** (eq 11). This presumably reflects both greater phosphine lability in **1c** and a more favorable equilibrium for formation of **10** from **1c**.

Solid-State Structures. The structures of **1a**, **1b**, **1d**, and **7a** (Figures 1−4, Tables 1−5) were determined by single crystal X-ray diffraction to be approximately octahedral. The steric congestion causes the two ostensibly trans PMe_3 ligands to tilt toward the smallest groups (RuH in **1a** and **1b**, RuH and $RuSiMe_2H$ in **1d**, and RuMe in **7a**; ∠P−Ru−P = 153.58(3)−167.3(1)°). The other two ligands cis to the smallest groups do not distort significantly in **1a**, **1b**, and **7a**; that is, the silyl and trans phosphine remain in essentially unperturbed octahedral positions (∠P−Ru−Si = 176.7(5)−177.63(3)°). The geometry

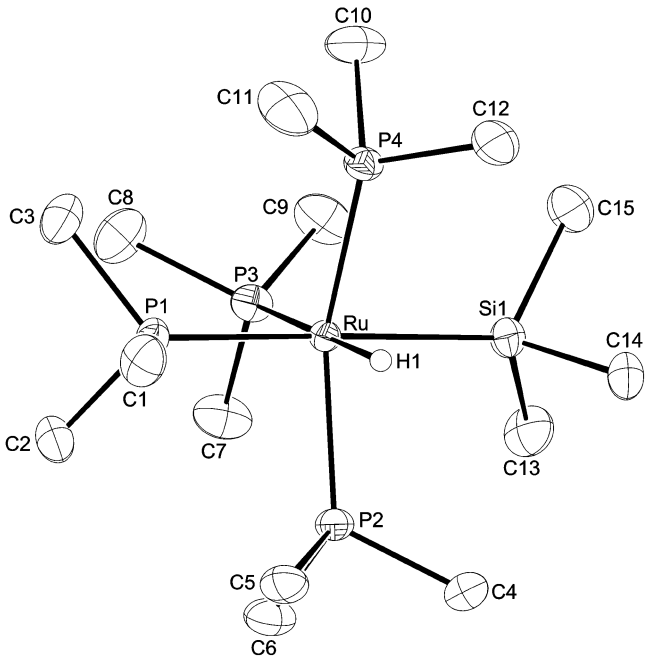

Figure 1. An ORTEP drawing of $(PMe_3)_4Ru(SiMe_3)H$, **1a** (30% thermal ellipsoids).

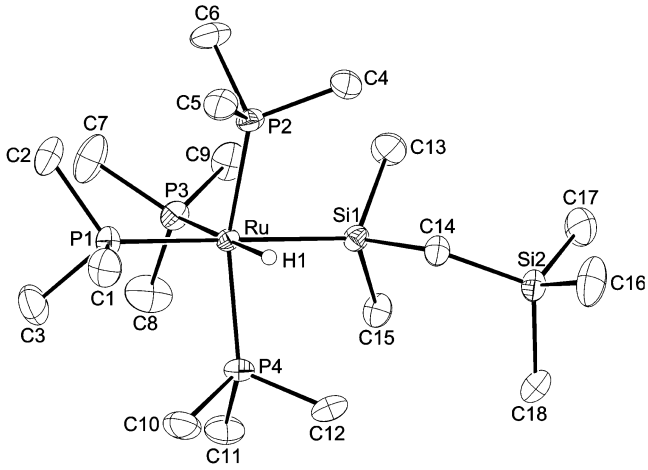

Figure 2. An ORTEP drawing of $(PMe_3)_4Ru(SiMe_2CH_2SiMe_3)H$, **1b** (30% thermal ellipsoids).

can be described as a distortion of the octahedron toward trigonal bipyramidal, tbp (ignoring the hydride or methyl ligands), with axial positions occupied by silyl and phosphine ligands. The structure of **1d**, on the other hand, is less crowded, and the steric pressure is relieved by a more uniform distortion of all ligands from the ideal octahedral positions. It is somewhat surprising that the relief of steric crowding in the hydrides **1a**, **1b**, and **1d** is not achieved by a closer approach of the hydride and silyl ligands and formation of a σ-SiH complex, as is found in many higher valent ruthenium silyl hydride complexes. This may be disfavored by the very electron-rich, formally Ru(0) centers that would result in the hypothetical $(PMe_3)_4Ru(\eta^2\text{-}HSiR_3)$. In any event, the structures of **1a**, **1b**, **1d**, and **7a** can be described as classical with all bond distances and angles within normal ranges. In all cases, the Ru−P distances trans to Si, H, and CH_3 ligands are the longest in a given complex. Such ground-state elongation of metal−ligand bonds trans to a strong σ-donor such as a silyl, hydride, and alkyl (trans influence) is well documented, and Nolan has correlated Ru−P bond length with

(43) Hartwig, J. F.; Andersen, R. A.; Bergman, R. G. *J. Am. Chem. Soc.* **1991**, *113*, 6492−6498.

Table 1. Crystal Data for **1a**, **1b**, **1d**, **4a**, and **7a**

compound	1a	1b	1d	4a	7a
formula	$C_{15}H_{46}P_4RuSi$	$C_{18}H_{54}P_4RuSi_2$	$C_{14}H_{44}P_4RuSi$	$C_{12}H_{39}P_3RuSi$	$C_{16}H_{48}P_4RuSi$
formula weight	479.68	551.74	465.56	405.52	493.58
crystal system	monoclinic	monoclinic	monoclinic	monoclinic	monoclinic
space group	*C*2/*c* (No. 15)	$P2_1/n$ (No. 14)	$P2_1/n$ (No. 14)	$P2_1/n$ (No. 14)	*C*2/*c* (No. 15)
color	colorless	colorless	colorless	colorless	colorless
Z	8	4	4	4	8
a, Å	15.5859(2)	12.3876(1)	9.113(1)	14.220(1)	15.2642(2)
b, Å	10.8807(1)	23.6973(3)	29.260(5)	9.802(3)	10.93880(10)
c, Å	29.6653(4)	10.2102(1)	9.353(2)	16.265(4)	31.0714(4)
β, deg	103.260(4)	97.801(1)	106.13(1)	96.67(1)	103.9820(10)
V, Å^3	4896.68(10)	2969.49(5)	2396(1)	2252(1)	5034.34(10)
T, K	210	227	227	296	200
R	0.0444[a]	0.0512[a]	0.049[b]	0.034[b]	0.0653[a]
w*R*	0.1024[a]	0.1035[a]	0.060[b]	0.039[b]	0.1295[a]
GOF	1.125	1.182	1.807	1.063	1.215

[a] All data used; $R = \sum(||F_o| - |F_c||)/\sum|F_o|$; $wR = \{\sum w(F_o^2 - F_c^2)^2/\sum w(F_o^2)^2\}^{1/2}$. [b] $F^2 > 3.0\sigma(F^2)$ data used; $R = \sum||F_o| - |F_c||/\sum|F_o|$; $wR = \{\sum w(|F_o| - |F_c|)^2/\sum w|F_o|^2\}^{1/2}$.

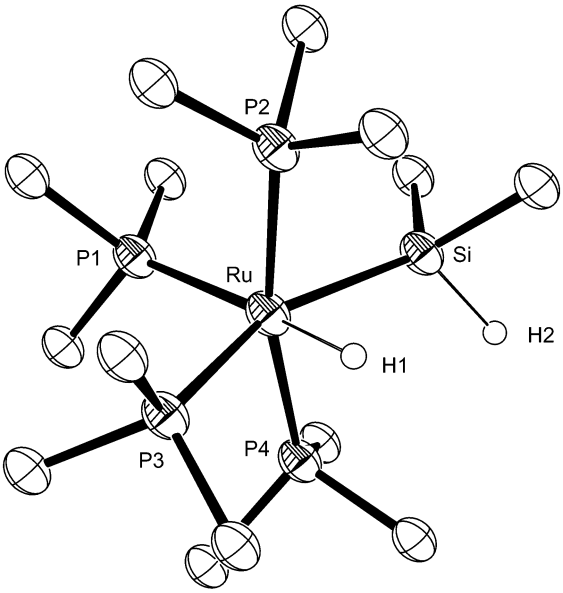

Figure 3. An ORTEP drawing of $(PMe_3)_4Ru(SiMe_2H)H$, **1d** (30% thermal ellipsoids).

Table 2. Selected Bond Distances and Nonbonding Contacts (Å) and Angles (deg) in **1a**

Ru−P1	2.3663(9)	Ru−P3	2.3561(9)	Ru−Si1	2.4630(9)
Ru−P2	2.3398(8)	Ru−P4	2.3060(8)	Ru−H1	1.59(4)
P2−Ru−P1	90.76(3)	P2−Ru−P3	103.81(3)		
P3−Ru−P1	92.91(3)	P2−Ru−P4	153.58(3)		
P4−Ru−P1	93.18(3)	P4−Ru−P3	102.07(3)		
P1−Ru−Si1	177.63(3)	P1−Ru−H1	90.2(10)		
P2−Ru−Si1	88.08(3)	P2−Ru−H1	75.0(14)		
P3−Ru−Si1	89.38(3)	P3−Ru−H1	176.7(10)		
P4−Ru−Si1	86.95(3)	P4−Ru−H1	78.8(14)		
Si1−Ru−H1	87.5(10)				

dissociation enthalpies in other complexes. It is, therefore, not surprising that the Ru−P distances in **1a**, **1b**, and **7a** are consistent with the qualitative trends for the kinetic and thermodynamic lability of the phosphines in these complexes.

The structure of the trihydride silyl **4a** was determined by the single-crystal X-ray diffraction method to be a seven-coordinate complex composed of a pseudo octahedral *fac*-$(PMe_3)_3RuH_3$ unit with the silyl group capping the face defined by the three hydride ligands (Figure 5, Tables 1 and 6). The hydride ligands were located and refined with isotropic thermal

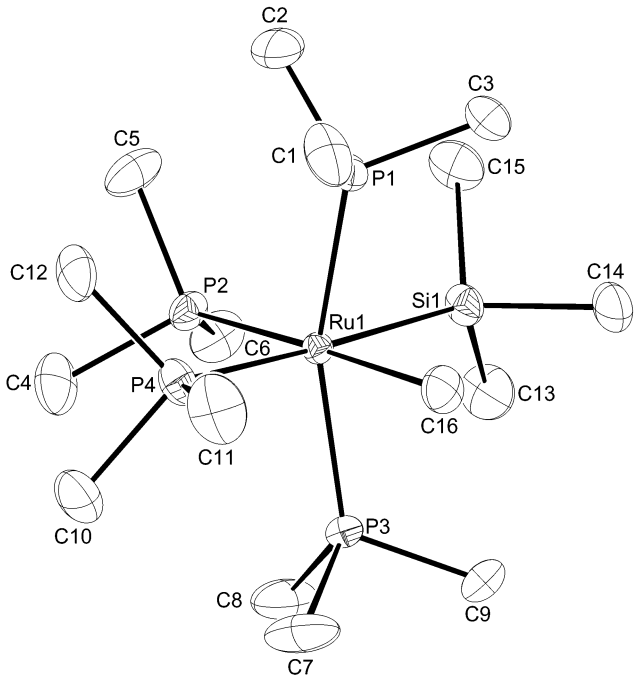

Figure 4. An ORTEP drawing of $(PMe_3)_4Ru(SiMe_3)Me$, **7a** (30% thermal ellipsoids).

Table 3. Selected Bond Distances and Nonbonding Contacts (Å) and Angles (deg) in **1b**

Ru−P1	2.3683(9)	Ru−P3	2.3591(8)	Ru−Si1	2.4796(9)
Ru−P2	2.3198(8)	Ru−P4	2.3222(8)	Ru−H1	1.61(4)
P2−Ru−P1	90.61(3)	P2−Ru−P3	102.74(3)		
P3−Ru−P1	92.08(3)	P2−Ru−P4	153.86(3)		
P4−Ru−P1	93.44(3)	P4−Ru−P3	102.90(3)		
P1−Ru−Si1	177.36(3)	P1−Ru−H1	91.4(12)		
P2−Ru−Si1	88.47(3)	P2−Ru−H1	77.8(12)		
P3−Ru−Si1	90.54(3)	P3−Ru−H1	176.5(12)		
P4−Ru−Si1	86.31(3)	P4−Ru−H1	76.3(12)		
Si1−Ru−H1	86.0(12)				

parameters. The Si−C and Ru−P bonds are eclipsed, and the hydride ligands are staggered with respect to the Si methyls and P atoms, yielding C_3 molecular symmetry. This ligand arrangement is typical for such $L_3M(ER_3)H_3$ (E = Si or Sn) complexes.[20,34−39,41,44] All heavy atom distances and angles are within the expected ranges. The formally nonbonded contacts

(44) Procopio, L. J. Ph.D. Thesis, University of Pennsylvania, 1991.

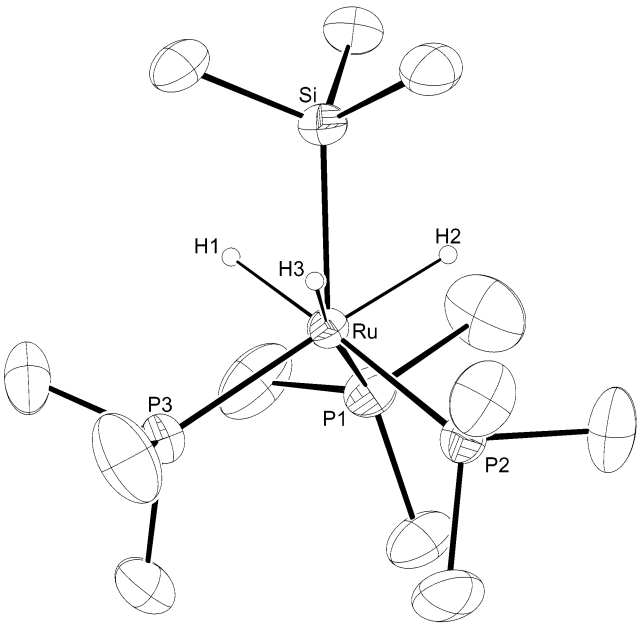

Figure 5. An ORTEP drawing of $(PMe_3)_3Ru(SiMe_3)H_3$, **4a** (30% thermal ellipsoids).

Table 4. Selected Bond Distances and Nonbonding Contacts (Å) and Angles (deg) in **1d**

Ru−P1	2.338(2)	Ru−P3	2.347(1)	Ru−Si1	2.426(1)
Ru−P2	2.328(2)	Ru−P4	2.316(2)	Ru−H1	1.524(58)
Si1−H2	1.523(79)	Si1···H1	2.675(50)		

P2−Ru−P1	93.4(1)	P2−Ru−P3	95.7(1)
P3−Ru−P1	100.2(1)	P2−Ru−P4	167.3(1)
P4−Ru−P1	95.1(1)	P4−Ru−P3	92.0(0)
P1−Ru−Si1	104.1(1)	P1−Ru−H1	173.9(19)
P2−Ru−Si1	86.0(1)	P2−Ru−H1	85.2(22)
P3−Ru−Si1	155.5(1)	P3−Ru−H1	74.1(18)
P4−Ru−Si1	82.8(1)	P4−Ru−H1	87.3(23)
Si1−Ru−H1	81.7(18)		

Table 5. Selected Bond Distances and Nonbonding Contacts (Å) and Angles (deg) in **7a**

Ru1−C16	2.215(6)	Ru1−P1	2.3680(13)	Ru1−P3	2.3181(12)
Ru1−Si1	2.4681(14)	Ru1−P2	2.3400(13)	Ru1−P4	2.3813(13)

P1−Ru1−P2	102.00(5)	C16−Ru1−P3	80.3(2)
P2−Ru1−P3	97.49(5)	C16−Ru1−P4	89.4(2)
P1−Ru1−P3	159.74(5)	C16−Ru1−Si1	89.9(2)
P1−Ru1−P4	90.47(5)	P1−Ru1−Si1	86.90(5)
P2−Ru1−P4	91.63(5)	P2−Ru1−Si1	89.11(5)
P3−Ru1−P4	94.47(5)	P3−Ru1−Si1	87.94(5)
C16−Ru1−P1	80.2(2)	P4−Ru1−Si1	177.36(5)
C16−Ru1−P2	177.6(2)		

between silicon and the ruthenium hydrides (2.13−2.23(5) Å) may indicate some delocalized bonding in the $Ru(Si)H_3$ fragment, albeit not as strong as typical agostic interactions (ca. 1.7−1.8 Å). The H···H separations (2.29−2.39(7) Å) are much longer than those found in η^2-H_2 and related complexes.[45] This is in accord with the solution spectroscopic data (T_1(25 °C) = 1500 ms at 200 MHz; IR (Nujol): ν(RuH) = 1890 cm^{-1}; $^1H\{^{31}P\}$ NMR (C_6D_6): J_{SiH} < 25 Hz). Evidence for nonclassical EH (E = Si or Sn) bonding, but not dihydrogen complexation, is also observed in other $L_3M(ER_3)H_3$ complexes, both in the solid state (X-ray) and in solution (J_{EH} and T_1 relaxation times).[35,37−39]

(45) Heinekey, D. M.; Oldham, W. J., Jr. *Chem. Rev.* **1993**, *93*, 913−926.

Table 6. Selected Bond Distances and Nonbonding Contacts (Å) and Angles (deg) in **4a**

Ru−P1	2.317(1)	Ru−H1	1.488(43)	Si···H1	2.228(42)
Ru−P2	2.320(1)	Ru−H2	1.637(50)	Si···H2	2.179(48)
Ru−P3	2.323(1)	Ru−H3	1.431(45)	Si···H3	2.128(48)
H1···H2	2.362(65)	H2···H3	2.287(66)	H1···H3	2.387(54)
Ru−Si	2.376(1)				

P1−Ru−P2	98.8(1)	P1−Ru−Si	118.5(1)
P2−Ru−P3	98.8(1)	P2−Ru−Si	118.0(1)
P1−Ru−P3	99.8(1)	P3−Ru−Si	119.0(1)
Si−Ru−H1	65.7(18)	P1−Ru−H1	75.2(19)
Si−Ru−H2	62.5(15)	P1−Ru−H2	79.3(16)
Si−Ru−H3	62.1(17)	P1−Ru−H3	173.5(16)
P2−Ru−H1	174.0(18)	P3−Ru−H1	82.7(17)
P2−Ru−H2	80.2(14)	P3−Ru−H2	178.5(15)
P2−Ru−H3	75.8(16)	P3−Ru−H3	84.9(18)
H1−Ru−H2	98.3(23)	H2−Ru−H3	95.9(24)
H1−Ru−H3	110.1(25)		

Discussion

Phosphine Lability in $(PMe_3)_4Ru(SiR_3)H$ Complexes. Reactions of **1a** with PMe_3-d_9, CO, and H_2 yield kinetically regiospecific trapping products, which are probably due to regiospecific phosphine dissociation from the site trans to Si and formation of the previously described five-coordinate 16e$^-$ intermediate with an empty site trans to Si.[29,30] It is possible that ligand dissociation might occur from one site to yield a fluxional intermediate, which is preferentially trapped at a different site. Fortunately, in the case of **1a**, this complication can be definitively excluded. Reaction of **1a-*d*$_9$** (labeled phosphine trans to silicon) with H_2 yields only **4a-*d*$_0$**, proving that phosphine dissociation is regiospecific. Furthermore, the reaction of **1a** with CO yields a kinetic product, ***mer*-8** (CO trans to silicon), proving that trapping with CO is also selective. Therefore, the regioselectivity of phosphine exchange in the site trans to silicon can indeed be taken at face value. A facile phosphine exchange in the position trans to silicon is also observed for the structurally related complexes **7a** and **1c**. It is reasonable to assume that the selective trapping is also due to selective dissociation, as is the case with the more thoroughly studied **1a**.

Exchange of the other phosphine sites in **1a**, **1c**, and **7a** with PMe_3-d_9 is always slower for a given complex than the exchange of the site trans to Si. The absolute rates, however, vary greatly between compounds and increase with steric congestion at the Ru center. Thus, the rate of exchange with PMe_3-d_9 of the other phosphines (i.e., not trans to silicon) follows this trend: **1a** (days) < **1c** < **7a** (minutes). Possible mechanisms for these exchanges include: (1) the slow dissociation of the less labile phosphines and immediate trapping; (2) trapping of minor geometrical isomers of a fluxional five-coordinate 16e$^-$ intermediate (e.g., **2a**); and (3) slow intramolecular rearrangement of the initial octahedral product. Although intramolecular isomerization is not common in octahedral geometries, it has been observed in some related complexes $(PR_3)_4MH_2$ (M = Fe, Ru, Os)[46−49] and $(CO)_4M(EMe_3)_2$ (M = Fe, Ru, Os; E = Si,

(46) Meakin, P.; Muetterties, E. L.; Tebbe, F. N.; Jesson, J. P. *J. Am. Chem. Soc.* **1971**, *93*, 4701.
(47) Tebbe, F. N.; Meakin, P.; Jesson, J. P.; Muetterties, E. L. *J. Am. Chem. Soc.* **1970**, *92*, 1068.
(48) Meakin, P.; Guggenberger, L. J.; Jesson, J. P.; Gerlach, D. H.; Tebbe, F. N.; Peet, W. G.; Muetterties, E. L. *J. Am. Chem. Soc.* **1970**, *92*, 3482.
(49) Muetterties, E. L. *Acc. Chem. Res.* **1970**, *3*, 266.

Ge, Sn, Pb),[50] as well as in the *mer* to *fac* rearrangement of the carbonyl compound ***mer*-8** to ***fac*-8** in the presence of PMe_3-d_9 (half-life of ca. 35 min at room temperature, vide supra). However, the increase in scrambling rates with increasing steric crowding in **1a**, **1c**, and **7a** would be also consistent with a dissociative mechanism.

The ability of silicon ligands to exert large trans effects has been noted previously in metal silyls,[51,52] including carbonyl complexes of ruthenium and osmium.[15−17,21] It is, therefore, not surprising that the ligands trans to Si in $(PMe_3)_4Ru(SiR_3)X$ complexes are considerably more labile than those adjacent to silicon. The magnitude of the effect is impressive, with most of the substitution reactions in the present studies approaching the fast regime on the NMR time scale. Alkyl and hydride groups are also strong trans directing ligands, but the phosphine trans to silicon in **1a**, **1c**, and **7a** is always the most labile by a substantial margin. The magnitude of silyl group trans effect can be put into perspective by considering two related complexes that do not contain silyl ligands: the cis dihydride **9** and the cis dimethyl complex **6**. Although hydride and methyl are generally considered strong trans directing ligands in their own right, **9** is quite inert to phosphine exchange below ca. 100 °C, and **6** exchanges with labeled phosphine only slowly at room temperature ($t_{1/2} \approx 10$ h). Thus, it is clear that steric and electronic effects combine to produce a dramatic, regioselective labilization of phosphines trans to silicon in octahedral silyl complexes.

In addition to the kinetic consequences, silyl ligands also induce weakening and elongation of the ruthenium−phosphine bonds trans to silicon in the ground-state structures. This "trans influence" is well established for metal silyl complexes, including those of Ru and Os.[21,22] The trans effect and trans influence are closely connected. Analysis of this relation is particularly instructive for series of structurally similar complexes such as **1a**, **1b**, and **7a**. In this series, the longest Ru−P bond within a complex is always trans to Si, and the second longest is trans to H. The most sterically crowded, **7a**, however, offers an interesting exception. The Ru−P bond trans to Si bond in **7a** is still the longest, and the bond trans to Me is also elongated, but not as much as one of the mutually trans Ru−P bonds. It is noteworthy that the relative elongation of Ru−P bonds in the ground state (trans influence) clearly parallels the lability of the ligands in question (trans effect). Thus, **1a** has only one Ru−P distance longer than 2.36 Å and exhibits exchange with PMe_3-d_9 selectively in that position. Indeed, exchange of this phosphine approaches the fast exchange regime on the NMR time scale at room temperature. Dissociation of the phosphine trans to silicon in **7a** is even more rapid, and this ruthenium−phosphorus distance is extremely long in the solid state (2.3813(13) Å). In this case, however, exchange of the other sites is relatively fast (minutes), consistent with another long Ru−P bond (2.3680(13) Å) observed in the solid-state structure. As a thermodynamic effect, the trans influence is also manifest in the position of dissociation equilibria and, therefore, in the abundance of the 16e$^-$ species produced by ligand dissociation. Indeed, the longest Ru−P bond (trans to silicon in **7a**) correlates with the greatest concentration of $(PMe_3)_3Ru(SiR_3)X$ in solution.

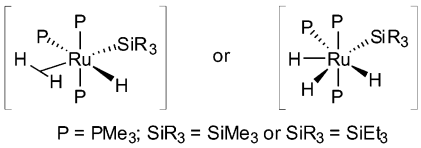

Figure 6. Possible high-energy meridianal isomers of compound **4**.

Scheme 1

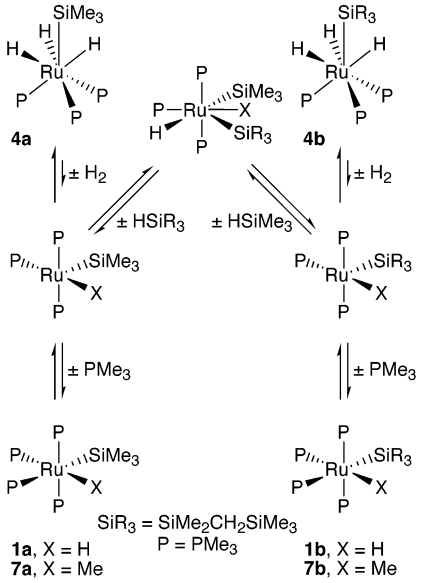

Lability of Dihydrogen in $(PMe_3)_3Ru(SiR_3)H_3$ Complexes. Elimination of dihydrogen from **4a** (and **4b**) is fast as is evident from the reactions with D_2, but the equilibrium lies strongly toward the trihydride complex in neat PMe_3, and it is difficult to increase the concentration of **1a** (and **1b**) even with the dynamic removal of the H_2 produced. Significantly, the traces of **1a**-d_9 produced by reaction of PMe_3-d_9 with **4a** exhibit the label in the position trans to silyl, even though the silyl ligand and all three hydrides are mutually cis in **4a**. Clearly, a rearrangement must occur, either prior to HH elimination from the seven-coordinate **4a** or subsequently in the five-coordinate intermediate, **2a**. The fact that HH elimination is very slow from the bulkier triethylsilyl complex **4c** is not consistent with a rate-limiting dissociative process, but rather suggests limiting isomerization to a sterically less favorable seven-coordinate species from which HH elimination occurs. One such species that can be envisioned would resemble the 16e$^-$ intermediate **2a**, but with two classical hydride ligands, or a single coordinated dihydrogen molecule filling the open coordination site (Figure 6). Presumably, the strong trans effect/influence of the silyl ligand would enhance HH bond formation and favor dissociation.

HH, SiH, CH, and SiC Reductive Eliminations from Seven-Coordinate Species. As shown above, 16e$^-$, five-coordinate species $(PMe_3)_3Ru(SiR_3)X$ are readily accessed from silyl complexes such as **1**, **4**, and **7**. The 16e$^-$ species, in turn, reversibly add SiH bonds to form 18e$^-$, seven-coordinate $(PMe_3)_3Ru(SiR_3)_2(X)H$ complexes (X = H[20] or Me, Scheme 1). Subsequent H−Si elimination and reassociation of phosphine or dihydrogen results in silyl group exchange (e.g., **1a** and **1b**, **7a** and **7b**, or **4a** and **4b**; Scheme 1). Silyl exchange is quite

(50) Vancea, L.; Pomeroy, R. K.; Graham, W. A. G. *J. Am. Chem. Soc.* **1976**, *98*, 1407.
(51) Azizian, H.; Dixon, K. R.; Eaborn, C.; Pidcock, A.; Shuaib, N. M.; Vinaixa, J. *J. Chem. Soc., Chem. Commun.* **1982**, 1020.
(52) Auburn, M. J.; Stobart, S. R. *Inorg. Chem.* **1985**, *24*, 318.

selective at room temperature, and ruthenium products arising from H_2, CH_4, $Me-SiMe_2CH_2SiMe_3$, or $Me-SiMe_3$ elimination pathways are not produced as readily. Again, bulkier silyl ligands inhibit the exchange rate, and reaction of **4c** with $HSiMe_3$ to produce the less hindered **4a** is very slow. This can be attributed to both the slow loss of H_2 from **4c** (vide supra) as well as the steric congestion in the requisite bis(silyl) dihydride intermediate, $(PMe_3)_3Ru(SiMe_3)(SiEt_3)(H)_2$. The latter factor is responsible for the sluggishness of the reverse reaction, **4a** with $HSiEt_3$, as H_2 loss from **4a** is facile.

Elimination of H_2 from $(PMe_3)_3Ru(SiR_3)(SiR_3')H_2$ has also been observed and leads to $(PMe_3)_3Ru(SiR_3)(SiR_3')$ species.[20] However, H_2 loss is much less favorable than silane loss, except in the case of small silanes such as $PhSiH_3$. Thus, productive dehydrogenative chemistry in these systems requires fairly high temperatures, or the removal of H_2 with hydrogen acceptors such as an olefin or even other $16e^-$ metal complex species. The other possible dissociative process from $(PMe_3)_3Ru(SiR_3)(SiR_3')H_2$ − SiSi elimination to produce R_3SiSiR_3' − has not been observed in these systems.

An interesting situation arises in the reaction of a hydridosilane with a complex containing an alkyl ligand, for example, **7a** + $HSiMe_3$, as the intermediate $(PMe_3)_3Ru(SiMe_3)_2(Me)H$ species can also undergo elimination of C−H and Si−C bonds. The SiH elimination is the fastest process, as evidenced by exchange with free silane with **7** on the NMR time scale at room temperature. At higher temperatures, however, both CH and SiC eliminations occur irreversibly, producing CH_4 and $SiMe_4$. In the case of the reaction of dimethyl complex **6** with silane, two methyl groups are ultimately extruded, and the CH_4 and $SiMe_4$ ratio of ca. 7:1 indicates a kinetic preference for CH elimination.

Activation of CH Bonds and H/D Exchange. The formation of the phenyl hydride complex **10** from **1a** and benzene could proceed via C−H activation by at least two different 16 e^- intermediates: the Ru(0) complex $(PMe_3)_4Ru$ formed by H−Si elimination or the Ru(II) complex **2a** formed by phosphine dissociation. The facts that deuterium exchange into **1a** is much faster than formation of **10** and that H/D exchange and formation of **10** are inhibited by added PMe_3 strongly suggest that phosphine dissociation is required. However, the formation of the intramolecular C−H activation product **5** is independent of phosphine concentration, and this species is produced by a separate (and minor) pathway involving the $(PMe_3)_4Ru$ species (Scheme 2, Path A).

Reaction of **2a** with benzene yields the $18e^-$ $(PMe_3)_3Ru(SiMe_3)(Ph)(H)_2$, as shown in Scheme 2, Path B. Note that analogues of this formally Ru(IV) intermediate, bis(silyl)-dihydride complexes $(PMe_3)_3Ru(SiMe_3)_2(H)_2$, have been isolated and structurally characterized.[20] The intermolecular CH oxidative addition of benzene to **2a** is rapidly reversible, which accounts for the faster rate of deuterium incorporation than formation of **10** in the case of reactions run in C_6D_6. Isotopic exchange would initially occur at the Ru−H position of **2a** (and hence **1a**), but subsequent and fast intramolecular C−H activation would lead to scrambling into the $SiMe_3$ and PMe_3 ligands via $(PMe_3)_3Ru(\eta^2\text{-}CH_2SiMe_2)(D)(H)$ (**3a-*d*$_1$**) and $(PMe_3)_2Ru(\eta^2\text{-}CH_2PMe_2)(SiMe_3)(D)(H)$. The former (**3a**) has been extensively studied and is actually slightly more stable than the $16e^-$ **2a**, although neither are stable in the presence of PMe_3 and revert to **1a**.[29,30]

Scheme 2

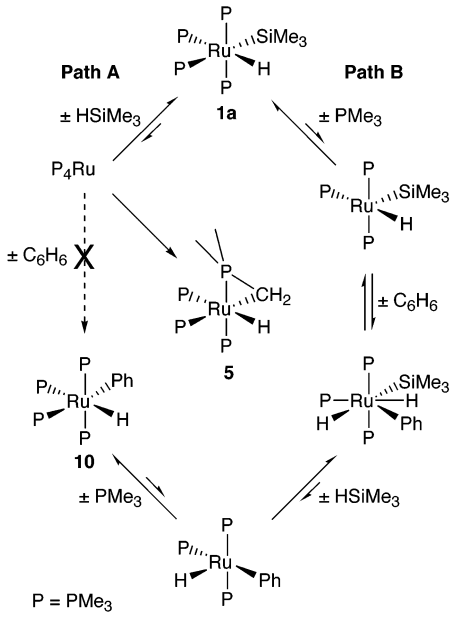

Although **5** could hypothetically arise from Me_3SiH loss from $(PMe_3)_2Ru(\eta^2\text{-}CH_2PMe_2)(SiMe_3)(H)_2$ and association of phosphine, this cannot be the primary path, as formation of **5** is not inhibited by added PMe_3, whereas H/D scrambling is. Thus, consistent with the extensive studies by Bergman,[43] Flood,[53,54] and their co-workers, **5** appears to arise from intramolecular C−H activation in $(PMe_3)_4Ru(0)$, whereas intermolecular C−H activation of benzene involves a Ru(II)/Ru(IV) reaction manifold. Formation of the phenyl complex **10** proceeds by the elimination of $HSiMe_3$ from $(PMe_3)_3Ru(SiMe_3)(Ph)(H)_2$ and trapping with phosphine, a process that is relatively slow as compared to benzene C−H (C−D) elimination and resultant H/D exchange. This is analogous to the H/D exchange between **10** and C_6D_6 reported by Bergman and shown to proceed via $(PMe_3)_3Ru(Ph)(C_6D_5)(D)H$. Similar pathways were described earlier by Flood and co-workers in the thermal conversion of $(PMe_3)_4Os(CH_2CMe_3)H$ into Os analogues of **5** and **10**.

Finally, it is worth noting that the faster rate for formation of **10** observed with the more hindered **1c** likely reflects both greater phosphine lability as compared to **1a** and a greater preference for $HSiEt_3$ loss from $(PMe_3)_3Ru(SiEt_3)(Ph)(H)_2$.

Relevance to Catalytic Dehydrocoupling and CH Functionalization. The reactivity trends reported above have direct implications for the SiC bond forming catalysis and allow for a number of conclusions. One of the key elements for any successful catalytic dehydrogenative (or dealkanative) SiC bond making process is the aptitude for the elimination of HH (or CH) and SiC bonds from the metal center. The present study illustrates that this aptitude can be greatly enhanced when the eliminating fragment is positioned trans to a silyl group, for example, a strong trans directing ligand. In octahedral or capped octahedral seven-coordinate complexes, simple geometrical

(53) Desrosiers, P. J.; Shinomoto, R. S.; Flood, T. C. *J. Am. Chem. Soc.* **1986**, *108*, 7964−7970.
(54) Desrosiers, P. J.; Shinomoto, R. S.; Flood, T. C. *J. Am. Chem. Soc.* **1986**, *108*, 1346−1347.

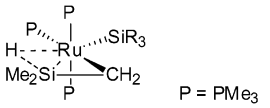

Figure 7. Possible high-energy meridianal isomer of $(PMe_3)_3Ru(\eta^2\text{-}CH_2SiMe_2)(SiMe_3)H$ with mutually trans silyl and agostic SiH ligands to promote SiC elimination.

arguments dictate that the two eliminating ligands and the trans directing silyl will be meridianal; thus, the remaining ligands must also be roughly meridianal. Indeed, such an orientation is found in the previously studied *mer*-$(PMe_3)_3Ru(SiMe_3)_2(H)_2$,[20] which is the true intermediate of the facile intermolecular SiH exchange observed for **1a**. This geometry is shared by those $(PMe_3)_3Ru(SiR_3)_2(H)_2$ ($SiR_3 = SiH_2Ph$ and $SiPh_2H$) complexes that exhibit fast SiH elimination.[20] When the meridianal structure is not accessible − such as in the chelating bis(silyl) complex $(PMe_3)_3Ru(SiMe_2CH_2CH_2SiMe_2)(H)_2$ − the SiH elimination is a very slow process.[20] It is reasonable to assume that SiH exchange in **1b**−**c**, **4a**−**c**, and **7a**−**c** (and CH/SiC eliminations in a reaction of **7a**−**c** with $HSiR_3$) also follows a path via *mer*-$(PMe_3)_3Ru(SiR_3)(SiR_3')(X)H$ intermediates (Scheme 1, X = H or Me). Note that the structures of these seven-coordinate intermediates are such that pairs of SiR_3 ligands are inequivalent, and elimination of only one type of SiR_3 group would be facilitated by a trans silyl. However, the previously reported dynamic exchange within pairs of H and SiR_3 ligands in these seven-coordinate species[20] yields accessible geometries for elimination of any SiH or SiC combination from a position trans to another silicon. The relative rate of SiC elimination remains slower than SiH elimination, due to the less favorable orbital overlap between the eliminating ligands (i.e., directional p-orbital of carbon vs spherical s-orbital of hydrogen). HH elimination from **4a**−**c** also proceeds via the *mer* isomer with HH trans to Si (Figure 6), and similar hypothetical structures can be drawn for HH and CH eliminations from $(PMe_3)_3Ru(SiR_3)(SiR_3')(X)H$ (X = H or Me).

It is noteworthy that the meridianal phosphine arrangement is also favorable for the 16e$^-$ **2a**,[29,30] a true intermediate in the SiC bond forming catalysis. The impact of meridianal phosphines is less obvious for the silyl silene species $(PMe_3)_3Ru(\eta^2\text{-}CH_2SiMe_2)(SiMe_3)H$, a long-postulated but never observed catalytic intermediate.[1,55] A facial phosphine arrangement was found for the ground state of the chemically related dihydride **3a**;[29,30] however, elimination could well occur from a slightly higher energy *mer* isomer. Indeed, both *fac* and *mer* isomers (95:5) were found for the hydrido chloride analogue, $(PMe_3)_3Ru(\eta^2\text{-}CH_2SiMe_2{-}H)Cl$.[56] The fine aspects of bonding might be somewhat different between the latter and **3a**, as the chloride derivative is better described as a β-agostic SiH complex rather than silene hydride. However, in a more general sense, existence of a *mer*-$(PMe_3)_3Ru(\eta^2\text{-}CH_2SiMe_2{-}H)Cl$ suggests a possibility of a *mer* isomer for the hydride derivative $(PMe_3)_3Ru(\eta^2\text{-}CH_2SiMe_2)(SiMe_3)H$ as well. For example, an isomer of $(PMe_3)_3Ru(\eta^2\text{-}CH_2SiMe_2)(SiMe_3)H$ with a mutually trans arrangement of silyl and "agostic SiH" ligands appears very reasonable on steric grounds (Figure 7) and should favor SiC elimination.

Although a meridianal tris-phosphine geometry is associated with faster rates of reductive elimination, this is not always the preferred geometry for a given complex. For example, the very stable ground-state structures of **4a**−**c** feature *fac*-phosphines, and this very stability inhibits catalytic chemistry in the system. It is, however, possible to enforce a meridianal structural motif by using chelating "pincer" phosphine ligands to avoid formation of excessively stable resting states for the catalyst. Another advantage of a *mer*-tris-phosphine ligand is that phosphine dissociation from such a rigid chelate would be very unlikely. We have recently observed facile phosphine dissociation from **2a** and formation of a plethora of bisphosphine intermediates.[20] The relevance of these species to the catalytic cycle is not known, but can be probed by the use of tridentate ligands. It would, therefore, appear promising for a number of reasons to attempt the use of "pincer" trisphosphine (or other tris-donor) ligands in dehydrogenative catalysis. These studies are currently underway and will be reported in the future.

Conclusions

Silyl complexes *cis*-$(PMe_3)_4Ru(SiR_3)H$ ($SiR_3 = SiMe_3$, **1a**; $SiMe_2CH_2SiMe_3$, **1b**; $SiEt_3$, **1c**; $SiMe_2H$, **1d**) and *cis*-$(PMe_3)_4Ru(SiR_3)Me$ ($SiR_3 = SiMe_3$, **7a**; $SiMe_2CH_2SiMe_3$, **7b**) adopt octahedral geometries in solution and the solid state with mutually cis silyl and hydride (or silyl and methyl) ligands. The longest Ru−P distance within each of the structurally characterized complexes (**1a**, **1c**, **1d**, and **7a**) is always trans to Si, reflecting the strong trans influence of silicon. Such phosphine ligands positioned trans to Si exhibit regioselective dissociation at a rate approaching the NMR time scale (trans effect of Si). In **7a**, the trans effect and trans influence are so strong that an equilibrium concentration of dissociated phosphine is detectable (∼5%) in solution of pure **7a**. Although dissociation of phosphine in **1a**−**c** is regioselective from the site trans to Si, the final products often result from intramolecular rearrangement and feature new ligands not trans, but cis to Si. Thus, oxidative addition of dihydrogen to **1a**−**c** furnishes hydrides cis to Si in the very stable *fac*-$(PMe_3)_3Ru(SiR_3)H_3$ ($SiR_3 = SiMe_3$, **4a**; $SiMe_2CH_2SiMe_3$, **4b**; $SiEt_3$, **4c**). The reverse manifold − HH elimination from **4a** and trapping with PMe_3 or PMe_3-d_9 − is also regioselective, but is very unfavorable. It appears to occur via a putative isomer of **4a** with two hydrides trans to a silyl and meridianal phosphine ligands (**1a**-d_9 is predominantly produced with PMe_3-d_9 trans to Si and *mer*-phosphine ligands). Slower, but irreversible, SiH elimination also occurs and ultimately furnishes $(PMe_3)_4RuH_2$ (**9**). The structure of **4a** exhibits a tetrahedral P_3Si environment around the metal with the three hydrides adjacent to silicon and capping the P_2Si faces. Although strong Si···HRu interactions are not indicated in the structure or by IR, the HSi distances (2.13−2.23(5) Å) suggest some degree of nonclassical SiH bonding in the H_3SiR_3 fragment. Thermolysis of **1a** in C_6D_6 at 45 °C leads to reversible intermolecular CD activation of C_6D_6 via an 18e$^-$ $(PMe_3)_3Ru(SiMe_3)(Ph\text{-}d_5)(H)(D)$ intermediate. Extensive H/D exchange into the hydride, $SiMe_3$, and PMe_3 ligands is observed, followed by much slower formation of *cis*-$(PMe_3)_4Ru(D)(Ph\text{-}d_5)$. The extensive H/D exchange into $SiMe_3$ and PMe_3 ligands occurs via $(PMe_3)_3Ru(\eta^2\text{-}CH_2SiMe_2)(D)(H)$ (**3a**-d_1) and $(PMe_3)_2Ru(\eta^2\text{-}CH_2PMe_2)(SiMe_3)(D)(H)$ intermediates. In an even slower intramolecular CH activation process, $(PMe_3)_3Ru(\eta^2\text{-}CH_2PMe_2)H$ is also produced by a separate (and minor) pathway involving the $(PMe_3)_4Ru$ species. The reactivity trends reported above illustrate that the HH, CH, and SiC elimination chemistry

(55) Berry, D. H.; Procopio, L. J. *J. Am. Chem. Soc.* **1989**, *111*, 4099−4100.
(56) Dioumaev, V. K.; Carroll, P. J.; Berry, D. H. *Angew. Chem.*, in press.

can be strongly enhanced by a trans directing silyl ligand. In octahedral or capped octahedral seven-coordinate complexes, simple geometrical arguments dictate that the two eliminating ligands and the trans directing silyl will be meridianal; thus, the remaining ligands must also be roughly meridianal. It is proposed to enforce a meridianal structural motif in the future generations of catalysts by using chelating "pincer" phosphine ligands to avoid the formation of excessively stable resting states (e.g., **4a**−**c**) and to enhance dehydrogenative and dealkanative catalytic activity.

Experimental Section

All manipulations were performed in Schlenk-type glassware on a dual-manifold Schlenk line or in a nitrogen-filled Vacuum Atmospheres glovebox. NMR spectra were obtained at 200- and 500-MHz (for ^{1}H) on Bruker AF-200 and AM-500 FT NMR spectrometers, respectively. All NMR spectra were recorded at 303 K unless stated otherwise. Chemical shifts are reported relative to tetramethylsilane for ^{1}H, ^{13}C, and ^{29}Si spectra, and external 85% H_3PO_4 for ^{31}P resonances. The temperature of the NMR probe was calibrated against methanol (estimated error 0.3 K). ^{13}C and ^{31}P NMR spectra were recorded with broadband ^{1}H decoupling. ^{29}Si NMR spectra were obtained using a DEPT-135 pulse sequence with ^{1}H refocusing. Spin−lattice relaxation times (T_1) were measured by using the standard inversion−recovery ($180° - \tau - 90°$) pulse sequence. Infrared spectra were recorded on a Perkin-Elmer model 1430 spectrometer. Elemental analyses were performed by Robertson Laboratory, Inc. (Madison, NJ). Photolysis reactions were carried out in a Rayonet photochemical reactor using low-pressure Hg arc lamps ($\lambda = 350$ nm).

Hydrocarbon solvents were dried over Na/K alloy-benzophenone. Benzene-d_6, cyclohexane-d_{12}, and methylcyclohexane-d_{14} were dried over Na/K alloy. H_2, D_2, and CO (Airco) were used as received. *cis*-$(PMe_3)_4RuMe_2$,[57] $(PMe_3)_3Ru(\eta^2\text{-}CH_2PMe_2)H$,[31,32] PMe_3,[58] and $HSiMe_2CH_2SiMe_3$[59] were synthesized according to the literature procedures. $HSiMe_3$ and $DSiMe_3$ were prepared by the reaction of Me_3SiCl and $LiAlH_4$ or $LiAlD_4$ in $^nBu_2O$ and purified by trap-to-trap vacuum fractionation. Triethylsilane (Aldrich) was dried over molecular sieves prior to use. PPh_3-polystyrene beads (Aldrich) were dried in vacuo. Triphenylborane (Aldrich) was recrystallized from hexanes/toluene before use.

Synthesis of *cis*-$(PMe_3)_4Ru(SiMe_3)Me$, 7a. A toluene (10 mL) solution of $(PMe_3)_4RuMe_2$ (1740 mg, 4.0 mmol) and $HSiMe_3$ (4.0 mmol) was stirred for 24 h at room temperature. The volatiles were removed in vacuo, and the residue was washed with cold pentane (−40 °C). Fractional recrystallization from toluene−pentane (1:10) yielded 250 mg (12.7% yield) of pure $(PMe_3)_4Ru(SiMe_3)Me$ as a white crystalline powder. ^{1}H NMR (C_6D_6): δ 1.18 (br s, 27H, P*Me*$_3$), 0.98 (d, $J_{PH} = 4.0$ Hz, 9H, P*Me*$_3$), 0.59 (s, 9H, Si*Me*$_3$), −0.37 (m, 3H, C*H*$_3$); (C_6D_{12}) δ 1.31 (br s, 27H, P*Me*$_3$), 1.28 (d, $J_{PH} = 4.4$ Hz, 9H, P*Me*$_3$), 0.14 (s, 9H, Si*Me*$_3$), −0.68 (m, 3H, C*H*$_3$). ^{13}C NMR (C_6D_6): δ 29.4 (m, P*Me*$_3$), 23.48 (m, P*Me*$_3$), 24.16 (d, $J_{PC} = 11.6$ Hz, *Me*), 12.47 (q, $J_{PC} = 3.0$ Hz, Si*Me*$_3$). ^{31}P NMR (C_6D_6): δ −3.0 (br m, 2P, mutually trans *P*Me$_3$), −14.5 (m, 1P, mutually cis *P*Me$_3$), −21.7 (br m, 1P, mutually cis *P*Me$_3$). Anal. Calcd for $C_{16}H_{48}Si_1P_4Ru_1$: C, 38.93; H, 9.80. Found: C, 38.88; H, 9.97.

VT ^{1}H NMR of $(PMe_3)_4Ru(SiMe_3)Me$, 7a. ^{1}H NMR (C_7D_8, 300 K): δ 1.19 (br s, 18H, P*Me*$_3$), 1.14 (br s, 9H, P*Me*$_3$), 1.01 (d, $J_{PH} = 4.5$ Hz, 9H, P*Me*$_3$), 0.49 (s, 9H, Si*Me*$_3$), −0.48 (m, 3H, C*H*$_3$); (C_7D_8, 240 K) δ 1.17 (br s, 18H, P*Me*$_3$), 1.11 (br s, 9H, P*Me*$_3$), 0.95 (d, $J_{PH} = 4.5$ Hz, 9H, P*Me*$_3$), 0.44 (s, 9H, Si*Me*$_3$), −0.41 (m, 3H, C*H*$_3$); (C_7D_8, 190 K) δ 1.16 (br s, 18H, P*Me*$_3$), 1.05 (br s, 9H, P*Me*$_3$), 0.88 (d, $J_{PH} = 4.5$ Hz, 9H, P*Me*$_3$), 0.81 (s, 9H, Si*Me*$_3$), −0.32 (m, 3H, C*H*$_3$). ^{31}P NMR (C_7D_8, 300 K): δ −4.10 (br s, 2P, mutually trans *P*Me$_3$), −15.65 (br s, 1P, mutually cis *P*Me$_3$), −22.80 (very br s, $\nu_{1/2} = 700$ Hz, 1P, mutually cis *P*Me$_3$); (C_7D_8, 240 K) δ −3.43 (dd, $J_{PP} = 29.6$ and 21.5 Hz, 2P, mutually trans *P*Me$_3$), −15.13 (q, $J_{PP} = 21.5$ Hz, 1P, mutually cis *P*Me$_3$), −20.28 (td, $J_{PP} = 29.6$ and 22.3 Hz, 1P, mutually cis *P*Me$_3$), −62.5 (s, free *P*Me$_3$); (C_7D_8, 190 K) δ −3.28 (dd, $J_{PP} = 29.6$ and 21.5 Hz, 2P, mutually trans *P*Me$_3$), −14.92 (q, $J_{PP} = 21.5$ Hz, 1P, mutually cis *P*Me$_3$), −19.88 (td, $J_{PP} = 29.6$ and 22.3 Hz, 1P, mutually cis *P*Me$_3$), −62.5 (s, free *P*Me$_3$).

Synthesis of *cis*-$(PMe_3)_4Ru(SiMe_3)H$, 1a. A cyclohexane solution (3 mL) of $(PMe_3)_4RuMe_2$ (2200 mg, 5.06 mmol) and $HSiMe_3$ (30.3 mmol) was stirred for 14 h at 60 °C in a bomb. The volatiles were removed in vacuo, and the residue was recrystallized from pentane to yield 2150 mg (89% yield) of pure $(PMe_3)_4Ru(SiMe_3)H$ as a white crystalline powder. ^{1}H NMR (C_6D_6): δ 1.33 (t, $J_{PH} = 2.0$ Hz, 18H, mutually trans P*Me*$_3$), 1.15 (d, $J_{PH} = 4.2$ Hz, 9H, mutually cis P*Me*$_3$), 1.13 (d, $J_{PH} = 4.9$ Hz, 9H, mutually cis P*Me*$_3$), 0.72 (d, $J_{PH} = 1.4$ Hz, 9H, Si*Me*$_3$), −11.17 (dtd, $J_{PH} = 66.5$, 31.9, and 15.5 Hz, 1H, Ru*H*); (C_6D_{12}) δ 1.38 (m, 27H, P*Me*$_3$), 1.25 (d, $J_{PH} = 5.0$ Hz, 9H, P*Me*$_3$), 0.22 (s, 9H, Si*Me*$_3$), −11.33 (dtd, $J_{PH} = 67.4$, 32.8, and 15.5 Hz, 1H, Ru*H*). ^{13}C NMR (C_6D_6): δ 28.5 (m, P*Me*$_3$), 28.0 (d, $J_{PC} = 15.1$ Hz, P*Me*$_3$), 16.6 (d, $J_{PC} = 2.5$ Hz, Si*Me*$_3$). ^{29}Si NMR (C_6D_6): δ 7.9 (dtd, $J_{PSi} = 97.6$, 26.0, 17.8 Hz, *Si*Me$_3$). ^{31}P NMR (C_6D_6): δ −4.8 (dd, $J_{PP} = 31$ and 25 Hz, 2P, mutually trans *P*Me$_3$), −15.2 (q, $J_{PP} = 25$ Hz, 1P, mutually cis *P*Me$_3$), −17.0 (q, $J_{PP} = 25$ Hz, 1P, mutually cis *P*Me$_3$). ^{31}P NMR (C_6D_{12}): δ −4.6 (dd, $J_{PP} = 31$ and 24 Hz, 2P, mutually trans *P*Me$_3$), −15.0 (q, $J_{PP} = 25$ Hz, 1P, mutually cis *P*Me$_3$), −16.6 (q, $J_{PP} = 27$ Hz, 1P, mutually cis *P*Me$_3$). IR (Nujol): ν(RuH) = 1821 cm^{-1}. IR (C_6H_6): ν(RuH) = 1827 cm^{-1}. Anal. Calcd for $C_{15}H_{46}Si_1P_4Ru_1$: C, 37.56; H, 9.67. Found: C, 37.82; H, 10.16.

Alternative Synthesis of *cis*-$(PMe_3)_4Ru(SiMe_3)H$, 1a. A benzene solution (15 mL) of $(PMe_3)_3Ru(\eta^2\text{-}CH_2PMe_2)H$ (550 mg, 1.36 mmol) and $HSiMe_3$ (2970 mg, 40.1 mmol) was photolyzed (350 nm) at 10 °C for 80.5 h. The volatiles were removed in vacuo, and the residue was recrystallized from petroleum ether, yielding 381 mg (59% yield) of $(PMe_3)_4Ru(SiMe_3)H$ as a white crystalline powder.

Synthesis of *cis*-$(PMe_3)_4Ru(SiMe_2CH_2SiMe_3)H$, 1b. A cyclohexane (2 mL) solution of $(PMe_3)_4RuMe_2$ (1.192 g, 2.74 mmol) and $HSiMe_2CH_2SiMe_3$ (1.6 mL, 13.7 mmol) was heated for 24 h at 60 °C. The volatiles were removed in vacuo, and the residue was recrystallized from pentane to yield 0.76 g (50.3%) of colorless crystals. ^{1}H NMR (C_6D_6): δ 1.32 (t, $J_{PH} = 2.4$ Hz, 18H, mutually trans P*Me*$_3$), 1.15 (d, $J_{PH} = 5.0$ Hz, 9H, mutually cis P*Me*$_3$), 1.13 (d, $J_{PH} = 5.0$ Hz, 9H, mutually cis P*Me*$_3$), 0.76 (d, $J_{PH} = 1.1$ Hz, 6H, Si*Me*$_2$), 0.39 (s, 9H, Si*Me*$_3$), 0.33 (s, 2H, C*H*$_2$), −11.21 (dtd, $J_{PH} = 67.5$, 32.8, and 16.4 Hz, 1H, Ru*H*); (C_6D_{12}) δ 1.39 (t, $J_{PH} = 2.3$ Hz, 18H, P*Me*$_3$), 1.38 (d, $J_{PH} = 1.8$ Hz, 9H, P*Me*$_3$), 1.25 (d, $J_{PH} = 5.5$ Hz, 9H, P*Me*$_3$), 0.33 (s, 6H, Si*Me*$_2$), 0.21 (d, $J_{PH} = 1.8$ Hz, 2H, C*H*$_2$), −0.01 (s, 9H, Si*Me*$_3$), −11.34 (dtd, $J_{PH} = 68.4$, 32.4, and 15.7 Hz, 1H, Ru*H*). ^{13}C NMR (C_6D_6): δ 28.4 (tt, $J_{PC} = 13.2$ and 4.0 Hz, P*Me*$_3$), 28.0 (dm, $J_{PC} = 16.0$ Hz, P*Me*$_3$), 17.8 (br s, C*H*$_2$), 16.4 (m, $J_{PC} = 3.2$ Hz, Si*Me*$_2$), 3.6 (s, Si*Me*$_3$). ^{29}Si NMR (C_6D_6): δ 11.05 (dm, $J_{PSi} = 83$ Hz, *Si*Me$_2$), 0.65 (d, $J_{PSi} = 5$ Hz, *Si*Me$_3$). ^{31}P NMR (C_6D_6): δ −5.64 (q, $J_{PP} = 29.2$ Hz, 2P, mutually *trans*-*P*Me$_3$), −15.74 (m, 1P, mutually *cis*-*P*Me$_3$), −17.27 (br m, 1P, mutually *cis*-*P*Me$_3$). IR (fluorolube): ν(RuH) = 1790 cm^{-1}. Anal. Calcd for $C_{18}H_{54}Si_2P_4Ru_1$: C, 39.18; H, 9.86. Found: C, 38.98; H, 9.85.

Synthesis of *cis*-$(PMe_3)_4Ru(SiEt_3)H$, 1c. A benzene solution (20 mL) of $(PMe_3)_3Ru(\eta^2\text{-}CH_2PMe_2)H$ (0.515 g, 1.270 mmol) and $HSiEt_3$ (3.02 g, 26.034 mmol) was photolyzed (350 nm) at 10 °C for 3 weeks. Volatiles were removed in vacuo, and the residue was recrystallized from petroleum ether, yielding 0.242 g of light brown $(PMe_3)_4Ru(SiEt_3)H$ (37% yield). ^{1}H NMR (C_6D_6): δ 1.42 (t, $J_{HH} = 7.8$ Hz, 6H, CH_2CH_3), 1.32 (t, $J_{PH} = 2.2$ Hz, 18H, two mutually trans P*Me*$_3$), 1.16

(57) Statler, J. A.; Wilkinson, G.; Thornton-Pett, M.; Hursthouse, M. B. *J. Chem. Soc., Dalton Trans.* **1984**, 1731.
(58) Luetkens, M. L.; Sattelberger, A. P.; Murray, H. H.; Basil, J. D.; Fackler, J. P. *Inorg. Synth.* **1989**, *26*, 7.
(59) Sakurai, H.; Hosomi, A.; Kumada, M. *Chem. Commun.* **1968**, 930.

(d, J_{PH} = 5.1 Hz, 9H, P*Me*$_3$), 1.14 (d, I_{PH} = 4.6 Hz, 9H, P*Me*$_3$), 1.04 (q, J_{HH} = 7.8 Hz, SiC*H*$_2$), −11.04 (dq, J_{PH} = 69.5 and 23.8 Hz, 1H, Ru*H*). ^{13}C NMR: δ 28.4 (m, P*Me*$_3$), 15.0 (CH$_2$*C*H$_3$), 11.0 (s, Si*C*H$_2$). ^{31}P NMR: δ −3.9 (t, J_{PP} = 30.9 Hz, 2P, two mutually trans *P*Me$_3$), −16.5 (q, $J_{PP} \approx$ 18 Hz, 1P, *P*Me$_3$), −19.9 (q, $J_{PP} \approx$ 21 Hz, 1P, *P*Me$_3$). IR (benzene): ν(RuH) = 1813 cm^{-1}. Anal. Calcd for $C_{18}H_{52}P_4Si_1Ru_1$: C, 41.44; H, 10.05. Found: C, 41.46; H, 9.61.

Synthesis of *cis*-(PMe$_3$)$_4$Ru(SiMe$_2$H)H, 1d. A cyclohexane solution (50 mL) of (PMe$_3$)$_4$Ru(H)$_2$ (**9**) (270 mg, 0.66 mmol) and Me$_2$SiH$_2$ (390 mg, 6.50 mmol) was photolyzed (350 nm) at 15 °C for 6 days. Volatiles were removed in vacuo, and the residue was recrystallized from petroleum ether at −40 °C to yield 240 mg (80%) of (PMe$_3$)$_4$Ru(SiMe$_2$H)H. ^{1}H NMR (C_6D_6): δ 4.60 (m, 1H, SiMe$_2$*H*), 1.35 (t, J_{HP} = 2.2 Hz, 18H, mutually trans P*Me*$_3$), 1.15 (d, J_{HP} = 3.6 Hz, 9H, mutually cis P*Me*$_3$), 1.13 (d, J_{HP} = 3.5 Hz, 9H, mutually cis P*Me*$_3$), 0.83 (d, J_{HP} = 4.0 Hz, 6H, Si*Me*$_2$H), −10.96 (dq, J_{HP} = 72 and 24 Hz, 1H, Ru*H*). ^{13}C NMR: δ 28.1 (d, J_{CP} = 15 Hz, P*Me*$_3$), 27.2 (d, J_{CP} = 18 Hz, P*Me*$_3$), 26.7 (t, J_{CP} = 14 Hz, P*Me*$_3$), 9.2 (s, Si*Me*$_2$H). ^{29}Si NMR δ −1.1 (dtd, J_{PSi} = 94, 28, 14 Hz, *Si*Me$_2$H). ^{31}P NMR δ −3.2 (t, J_{HP} = 29 Hz, 2P, two mutually trans *P*Me$_3$), −14.3 (m, 1P, *P*Me$_3$), −16.5 (m, 1P, *P*Me$_3$). Anal. Calcd for $C_{14}H_{44}SiP_4Ru_1$: C, 36.12; H, 9.53. Found: C, 36.58; H, 9.73.

Synthesis of *cis*-(PMe$_3$)$_4$RuH$_2$, 9. A cyclohexane solution (10 mL) of (PMe$_3$)$_3$Ru(η^2-CH$_2$PMe$_2$)H (0.797 g, 1.966 mmol) was placed in a thick-walled glass pressure flask, and PMe$_3$ (1.45 mmol) was added by vacuum transfer at −196 °C. The solution was placed under 3 atm H_2 and heated at 110 °C for 91 h. Volatiles were removed in vacuo, and the pale yellow residue was sublimed (85 °C, 10^{-4} Torr), yielding 0.702 g of white *cis*-(PMe$_3$)$_4$RuH$_2$ (88% yield). Spectroscopic data are in agreement with literature values.[60,61] ^{1}H NMR (C_6D_{12}): δ 1.32 (t, J_{PH} = 2.5 Hz, 18H, mutually trans P*Me*$_3$), 1.28 (d, J_{PH} = 4.6 Hz, 18H, PMe$_3$), −10.09 (m, RuH$_2$). IR (benzene): ν(RuH) = 1820 cm^{-1}.

Reaction of (PMe$_3$)$_4$Ru(SiMe$_3$)H and PMe$_3$-*d*$_9$. An NMR tube was loaded with a C_6D_6 solution (0.5 mL) of (PMe$_3$)$_4$Ru(SiMe$_3$)H (11 mg, 0.023 mmol), and the solution was degassed in vacuo. At −196 °C, PMe$_3$-*d*$_9$ (0.35 mmol) was added, and the tube was sealed. Upon thawing, ^{1}H and ^{31}P NMR spectra were recorded, showing complete exchange of only the phosphine ligand in the position trans to silicon within 2 min. The other phosphine ligands are exchanging with free phosphine with a $\tau_{1/2}$ of ca. 2 days. ^{31}P NMR (C_6D_6): δ −5.22 (dd, J_{PP} = 31 and 25 Hz, mutually trans *P*Me$_3$), −5.88 (dd, J_{PP} = 31 and 25 Hz, PMe$_3$ trans to *P*Me$_3$-*d*$_9$), −6.80 (dd, J_{PP} = 31 and 25 Hz, PMe$_3$-*d*$_9$ trans to *P*Me$_3$), −7.40 (dd, J_{PP} = 31 and 25 Hz, mutually trans PMe$_3$-*d*$_9$), −15.56 (m, *P*Me$_3$ trans to H), −17.45 (m, *P*Me$_3$-*d*$_9$ trans to H), −19.85 (m, PMe$_3$-*d*$_9$ trans to Si).

Reaction of (PMe$_3$)$_4$Ru(SiMe$_3$)Me and PMe$_3$-*d*$_9$. An NMR tube was loaded with a C_6D_6 solution (0.5 mL) of (PMe$_3$)$_4$Ru(SiMe$_3$)Me (10 mg, 0.02 mmol), and the sample was degassed in vacuo. At −196 °C, PMe$_3$-*d*$_9$ (0.24 mmol) was added, and the tube was sealed. Upon thawing, the reaction was followed by ^{1}H and ^{31}P NMR spectroscopy. After only 3 min, all phosphine positions showed nonselective incorporation of labeled phosphine (^{1}H NMR: 40% deuterium in the mutually trans positions at δ 1.21 and 30% in the position at δ 1.11). The ^{1}H (δ 0.98) and ^{31}P (δ −21.7) resonances for one of the mutually cis phosphines disappeared due to coalescence with free phosphine signal. After 1 day, statistical distribution of 76% deuterium is found in all observable positions including free phosphine (^{1}H and ^{31}P NMR). ^{1}H NMR (C_6D_6): δ 1.20 and 1.18 (br s, 18H, mutually trans P*Me*$_3$ and P*Me*$_3$ trans to PMe$_3$-*d*$_9$), 1.11 (d, J_{PH} = 5.2 Hz, 9H, P*Me*$_3$ trans to H), 0.79 (d, J_{PH} = 1.9 Hz, free P*Me*$_3$), 0.59 (s, 9H, Si*Me*$_3$), −0.41 (m, 3H, C*H*$_3$). ^{31}P NMR (C_6D_6): δ −3.80 (d, J_{PP} = 21.5 Hz, mutually trans *P*Me$_3$), −4.60 (d, J_{PP} = 21.5 Hz, PMe$_3$ trans to *P*Me$_3$-*d*$_9$), −5.45 (d, J_{PP} = 21.9 Hz, PMe$_3$-*d*$_9$ trans to *P*Me$_3$), −6.16 (d, J_{PP} = 21.5 Hz, mutually trans PMe$_3$-*d*$_9$), −15.46 (t, J_{PP} = 21.6 Hz, *P*Me$_3$ trans to H), −17.77 (t, J_{PP} = 21.6 Hz, PMe$_3$-*d*$_9$ trans to H).

Reaction of *cis*-(PMe$_3$)$_4$Ru(SiEt$_3$)H and PMe$_3$-*d*$_9$. An NMR tube was loaded with a C_6D_6 solution (0.5 mL) of *cis*-(PMe$_3$)$_4$Ru(SiEt$_3$)H (6 mg, 0.012 mmol) and placed under vacuum. At −196 °C, PMe$_3$-*d*$_9$ (0.17 mmol) was added, and the tube was sealed. Upon thawing, the ^{1}H NMR spectrum was recorded within 5 min, confirming that ca. 1 equiv of deuterated phosphine had been incorporated into *cis*-(PMe$_3$)$_4$Ru(SiEt$_3$)H. After 1 h at 25 °C, the ^{1}H NMR spectrum showed that complete exchange with all positions had occurred.

Photolytic Reaction of (PMe$_3$)$_3$Ru(η^2-CH$_2$PMe$_2$)H and PMe$_3$-*d*$_9$. An NMR tube was loaded with a C_6D_6 solution (0.5 mL) of (PMe$_3$)$_3$Ru(η^2-CH$_2$PMe$_2$)H (17 mg, 0.042 mmol) and placed under vacuum. PMe$_3$-*d*$_9$ (0.4 mmol) was added, and the tube was sealed. The tube was photolyzed (λ = 350 nm) at 10 °C, and the reaction was monitored by ^{1}H NMR. After 24 h, ca. 20% exchange of the PMe$_3$ ligands for PMe$_3$-*d*$_9$ had occurred.

Thermal Reaction of (PMe$_3$)$_3$Ru(η^2-CH$_2$PMe$_2$)H and PMe$_3$-*d*$_9$. An NMR tube was loaded with a C_6D_{12} solution (0.5 mL) of (PMe$_3$)$_3$Ru(η^2-CH$_2$PMe$_2$)H (15 mg, 0.037 mmol) and C_6Me_6 (2 mg, internal standard) and placed under vacuum. PMe$_3$-*d*$_9$ (0.44 mmol) was added, and the tube was sealed. The tube was heated at 65 °C, and the reaction was monitored by ^{1}H NMR. After 102 h, ca. 50% exchange of the PMe$_3$ ligands for PMe$_3$-*d*$_9$ had occurred.

Attempted Reaction of (PMe$_3$)$_4$Ru(SiMe$_3$)Me with BPh$_3$. BPh$_3$ (19 mg, 0.04 mmol) and (PMe$_3$)$_4$Ru(SiMe$_3$)Me (40 mg, 0.12 mmol) were suspended in 1 mL of pentane. A color change from light orange to dark red and formation of a white precipitate started within seconds. The mixture was stirred for 10 min, filtered, and stirred with 40 mg of polymer-supported PPh$_3$ (cross-linked polystyrene beads, 3 mmol of PPh$_3$ per 1 g of polymer) for 10 min, decanted, treated again with 10 mg of PPh$_3$-polystyrene beads, and decanted again. The volatiles were removed in vacuo, the solids were redissolved in C_6D_{12}, and the sample was sealed in an NMR tube under ca. 1 atm of N_2.

Observation of *mer*-(CO)(PMe$_3$)$_3$Ru(SiMe$_3$)H, *mer*-8. An NMR tube was loaded with a C_6D_6 solution (0.5 mL) of (PMe$_3$)$_4$Ru(SiMe$_3$)H (17 mg, 0.035 mmol), and the solution was degassed in vacuo. At −196 °C, carbon monoxide (ca. 0.30 mmol) was added, and the tube was sealed. The mixture was thawed to room temperature, and the ^{1}H and ^{31}P NMR spectra were recorded within 10 min. Initial spectra showed only the presence of *mer*-(CO)(PMe$_3$)$_3$Ru(SiMe$_3$)H and PMe$_3$. The isomerization to *fac*-(CO)(PMe$_3$)$_3$Ru(SiMe$_3$)H (***fac*-8**) was followed by ^{1}H NMR spectroscopy. After 36 min at 25 °C, the tube contained a 1:1 mixture of *fac* and *mer* isomers. The *fac*/*mer* system came to a 95:5 equilibrium within 12 h.

***mer*-(CO)(PMe$_3$)$_3$Ru(SiMe$_3$)H.** ^{1}H NMR (C_6D_6): δ 1.29 (t, J_{PH} = 2.8 Hz, 18H, mutually trans P*Me*$_3$), 1.10 (d, J_{PH} = 6.3 Hz, 9H, P*Me*$_3$), 0.51 (s, 9H, Si*Me*$_3$), −9.07 (dt, J_{PH} = 73.8 and 29.1 Hz, 1H, Ru*H*, trans to CO). ^{31}P NMR (C_6D_6): δ −7.0 (d, J_{PP} = 23 Hz, 2P, mutually trans *P*Me$_3$), −15.7 (t, J_{PP} = 23 Hz, 1P, *P*Me$_3$, trans to hydride).

Synthesis of *fac*-(CO)(PMe$_3$)$_3$Ru(SiMe$_3$)H, *fac*-8. A C_6H_6 solution (20 mL) of (PMe$_3$)$_4$Ru(SiMe$_3$)H (385 mg, 0.80 mmol) was stirred under 1 atm of carbon monoxide for 2.5 h. Volatiles were removed in vacuo, and the residue was recrystallized from petroleum ether, yielding 294 mg (85% yield) of a mixture of *fac*- and *mer*-(CO)(PMe$_3$)$_3$Ru(SiMe$_3$)H in a 95:5 ratio. ^{1}H NMR (C_6D_6): δ 1.123 (d, J_{PH} = 6.3 Hz, 9H, P*Me*$_3$), 1.117 (d, J_{PH} = 6.3 Hz, 9H, P*Me*$_3$), 1.09 (d, J_{PH} = 7.0 Hz, 9H, P*Me*$_3$), 0.71 (d, J_{PH} = 1.3 Hz, 9H, Si*Me*$_3$), −9.11 (ddd, J_{PH} = 67.1, 29.9, and 21.4 Hz, 1H, Ru*H*). ^{13}C NMR (C_6D_6): δ 207.9 (dt, J_{PC} = 79.3 and 9.0 Hz, *C*O), 25.4 (d, J_{PC} = 19.5 Hz, P*Me*$_3$), 24.5 (td, J_{PC} = 24.2 and 5.0 Hz, P*Me*$_3$), 24.2 (d, J_{PC} = 21.3 Hz, P*Me*$_3$), 12.9 (s, Si*Me*$_3$). ^{29}Si NMR (C_6D_6): δ 4.6 (ddd, J_{PSi} = 74.8, 21.0, 11.3 Hz, *Si*Me$_3$). ^{31}P NMR (C_6D_6): δ −11.2 (t, J_{PP} = 37 Hz, 1P, *P*Me$_3$), −15.9 (dd, J_{PP} = 37 and 21 Hz, 1P, *P*Me$_3$), −22.0 (dd, J_{PP} = 37 and 21 Hz, 1P, *P*Me$_3$). IR (C_6H_6): ν(CO) = 1932 cm^{-1}, ν(RuH) = 1858 cm^{-1}. Anal. Calcd for $C_{13}H_{37}O_1Si_1P_3Ru_1$: C, 36.19; H, 8.64. Found: C, 36.10; H, 8.83.

(60) Jones, R. A.; Wilkinson, G.; Colquohoun, I. J.; McFarlane, W.; Galas, A. M. R.; Hursthouse, M. B. *J. Chem. Soc., Dalton Trans.* **1980**, 2480.
(61) Mainz, V. V.; Andersen, R. A. *Organometallics* **1984**, *3*, 675.

Isomerization of *mer*-(CO)(PMe_3)$_3$Ru($SiMe_3$)H in the Presence of PMe_3-d_9. A C_6H_6 solution (1 mL) of (PMe_3)$_4$Ru($SiMe_3$)H (10 mg, 0.02 mmol) was stirred under ca. 3 atm of CO for 5 min. The excess of CO was removed in vacuo, and PMe_3-d_9 (0.40 mmol) was added. The solution was stirred in the dark for 1 h, and volatiles were removed in vacuo. ^{1}H and ^{31}P spectra showed no incorporation of PMe_3-d_9 into the final product, *fac*-(CO)(PMe_3)$_3$Ru($SiMe_3$)H.

Reaction of (PMe_3)$_4$Ru($SiMe_3$)Me with $HSiMe_2CH_2SiMe_3$. An NMR tube was loaded with a C_6D_6 solution (0.5 mL) of (PMe_3)$_4$Ru($SiMe_3$)Me (10 mg, 0.02 mmol). $HSiMe_2CH_2SiMe_3$ (0.20 mmol) was vacuum transferred into the tube, and the tube was flame sealed. The ^{1}H NMR spectra were recorded after 0.2, 2, and 48 h to verify establishment of the equilibrium. The equilibrium constant (K_{eq}(300) = 0.0059) was recalculated from the integral intensities of the ^{1}H NMR signals of (PMe_3)$_4$Ru($SiMe_3$)Me, (PMe_3)$_4$Ru($SiMe_2CH_2SiMe_3$)Me, $HSiMe_3$, and $HSiMe_2CH_2SiMe_3$.

(PMe_3)$_4$Ru($SiMe_2CH_2SiMe_3$)Me. ^{1}H NMR (C_6D_6): δ 1.17 (br s, 27H, P*Me*$_3$), 0.99 (d, J_{PH} = 2.5 Hz, 9H, P*Me*$_3$), 0.54 (s, 6H, Si*Me*$_2$), 0.30 (s, 9H, Si*Me*$_3$), 0.20 (s, 2H, C*H*$_2$), −0.15 (m, 3H, Ru*Me*).

Reaction of (PMe_3)$_4$Ru($SiMe_3$)H with $HSiMe_2CH_2SiMe_3$. An NMR tube was loaded with a C_6D_6 solution (0.5 mL) of (PMe_3)$_4$Ru($SiMe_3$)H (10 mg, 0.02 mmol). $HSiMe_2CH_2SiMe_3$ (0.20 mmol) was vacuum transferred into the tube, and the tube was flame sealed. The ^{1}H NMR spectra were recorded after 2 min and 48 h to verify establishment of the equilibrium. The equilibrium constant (K_{eq}(300) = 0.0065) was recalculated from the integral intensities of the ^{1}H NMR signals of (PMe_3)$_4$Ru($SiMe_3$)H, (PMe_3)$_4$Ru($SiMe_2CH_2SiMe_3$)H, $HSiMe_3$, and $HSiMe_2CH_2SiMe_3$.

Reaction of (PMe_3)$_4$Ru($SiMe_3$)H with $DSiMe_3$. An NMR tube was loaded with a C_6D_6 solution (0.5 mL) of (PMe_3)$_4$Ru($SiMe_3$)H (24 mg, 0.05 mmol). $DSiMe_3$ (0.5 mmol) was vacuum transferred into the tube, and the tube was flame sealed. The ^{1}H NMR spectrum was recorded within 5 min and showed complete conversion to (PMe_3)$_4$Ru($SiMe_3$)D, with the generation of ca. 1 equiv of free $HSiMe_3$.

Thermolysis of (PMe_3)$_4$Ru($SiMe_3$)H in C_6D_{12}. An NMR tube was loaded with a C_6D_{12} solution (0.5 mL) of (PMe_3)$_4$Ru($SiMe_3$)H (5 mg, 0.01 mmol) and C_6Me_6 (2 mg, internal standard), the solution was degassed in vacuo, and the tube was sealed. The sample was heated at 65 °C, and the reaction was monitored by ^{1}H NMR spectroscopy. The reaction proceeded to yield (PMe_3)$_3$Ru(η^2-CH_2PMe_2)H and free $HSiMe_3$ over a period of several days.

Thermolysis of (PMe_3)$_4$Ru($SiMe_3$)H in C_6H_6 − Synthesis of *cis*-(PMe_3)$_4$Ru(Ph)H. A benzene solution (30 mL) of (PMe_3)$_4$Ru($SiMe_3$)H (275 mg, 0.57 mmol) was heated at 65 °C for a total of 348 h. To prevent the buildup of $HSiMe_3$, the volatiles were periodically removed in vacuo, and fresh benzene was added. The reaction was monitored by ^{1}H NMR spectroscopy. Volatiles were removed in vacuo, and the residue was recrystallized from petroleum ether to yield 220 mg of pale orange (PMe_3)$_4$Ru(Ph)H (79% yield). ^{1}H NMR (C_6D_6): δ 7.99 and 7.11 (m, 5H, Ph), 1.20 (d, J_{PH} = 4.6 Hz, 9H, mutually cis PMe_3), 1.16 (d, J_{PH} = 5.4 Hz, 9H, mutually cis PMe_3), 1.08 (t, J_{PH} = 2.7 Hz, 18H, mutually trans PMe_3), −9.41 (dq, J_{PH} = 94.0 and 26.3 Hz, 1H, RuH). ^{13}C NMR (C_6D_{12}): δ 125.5 (br s, Ph), 120.4 (br s, Ph), 29.0 (d, J_{PC} = 16 Hz, PMe_3), 25.6 (d, J_{PC} = 17 Hz, P*Me*$_3$), 24.6 (m, mutually trans P*Me*$_3$). ^{31}P NMR (C_6D_6): δ −1.9 (t, J_{PP} = 26 Hz, 2P, mutually trans *P*Me$_3$), −11.0 (dt, J_{PP} = 26 and 18 Hz, 1P, *P*Me$_3$, trans to Ph), −17.6 (dt, J_{PP} = 26 and 18 Hz, 1P, *P*Me$_3$, trans to hydride). IR (Nujol): ν(RuH) = 1855 cm^{-1}. Anal. Calcd for $C_{18}H_{42}P_4Ru_1$: C, 44.72; H, 8.76. Found: C, 44.32; H, 8.98.

Thermolysis of *cis*-(PMe_3)$_4$Ru($SiEt_3$)H in C_6H_6. A benzene solution (0.8 mL) of *cis*-(PMe_3)$_4$Ru($SiEt_3$)H (15 mg, 0.029 mmol) was heated at 65 °C for 50 h, and the volatiles were removed in vacuo. The ^{1}H NMR spectrum of the solid residues showed complete conversion to *cis*-(PMe_3)$_4$Ru(Ph)H (>85%) and several other minor products, including (PMe_3)$_3$Ru(η^2-CH_2PMe_2)H (ca. 5%).

Reaction of (PMe_3)$_4$Ru($SiMe_3$)H with H_2. An NMR tube was loaded with a C_6D_6 solution (0.5 mL) of (PMe_3)$_4$Ru($SiMe_3$)H (9 mg, 0.02 mmol), and the sample was degassed in vacuo. Hydrogen (ca. 3 atm) was added, and the tube was sealed. The ^{1}H NMR spectrum was recorded within 5 min and showed complete conversion to (PMe_3)$_3$Ru($SiMe_3$)H_3, with the generation of ca. 1 equiv of free PMe_3.

Synthesis of (PMe_3)$_3$Ru($SiMe_3$)H_3, 4a. Method 1: A cyclohexane solution (20 mL) of *cis*-(PMe_3)$_4$RuH_2 (0.500 g, 1.23 mmol) and $HSiMe_3$ (0.900 g, 12.16 mmol) was photolyzed (350 nm) at 10 °C for 87 h. Volatiles were removed in vacuo, and the residue was recrystallized from petroleum ether, yielding 0.442 g of colorless (PMe_3)$_3$Ru($SiMe_3$)H_3 (89% yield).

Method 2: A benzene solution (50 mL) of (PMe_3)$_4$Ru($SiMe_3$)H (1.491 g, 3.11 mmol) was stirred under 3.5 atm hydrogen for 20 h. Volatiles were removed in vacuo, and the residue was recrystallized from petroleum ether, yielding 0.822 g of colorless (PMe_3)$_3$Ru($SiMe_3$)H_3 (65% yield).

^{1}H NMR (C_6D_6): δ 1.13 (m, 27H, P*Me*$_3$), 0.90 (s, 9H, Si*Me*$_3$), −10.18 (br m, 3H, Ru*H*$_3$); (C_6D_{12}) δ 1.32 (m, 27H, P*Me*$_3$), 0.30 (s, 9H, Si*Me*$_3$), −10.34 (br m, 3H, Ru*H*$_3$). ^{13}C{^{1}H} NMR (C_6D_6): δ 26.7 (m, P*Me*$_3$), 18.8 (d, $^3J_{PC}$ = 3.3 Hz, Si*Me*$_3$). ^{29}Si NMR (C_6D_6): δ −10.8 (q, $^2J_{PSi}$ = 7.6 Hz, *Si*Me$_3$). ^{31}P{^{1}H} NMR (C_6D_6): δ −5.0 (s, *P*Me$_3$). ^{31}P{^{1}H} NMR (C_6D_{12}): δ −4.5 (s, *P*Me$_3$). IR (Nujol): ν(RuH) = 1890 cm^{-1}. IR (benzene): ν(RuH) = 1887 cm^{-1}. Anal. Calcd for $C_{12}H_{39}P_3SiRu$: C, 35.54; H, 9.69. Found: C, 35.36; H, 10.02.

Synthesis of (PMe_3)$_3$Ru($SiMe_2CH_2SiMe_3$)H_3, 4b. A benzene solution (25 mL) of *cis*-(PMe_3)$_4$RuH_2 (0.500 g, 1.23 mmol) and $HSiMe_2CH_2SiMe_3$ (0.843 g, 5.77 mmol) was photolyzed (350 nm) at 10 °C for 167 h. Volatiles were removed in vacuo, and the residue was recrystallized from petroleum ether, yielding 0.540 g of colorless (PMe_3)$_3$Ru($SiMe_2CH_2SiMe_3$)H_3 (92% yield).

Synthesis of (PMe_3)$_3$Ru($SiEt_3$)H_3, 4c. A benzene solution (25 mL) of *cis*-(PMe_3)$_4$RuH_2 (0.313 g, 0.768 mmol) and $HSiEt_3$ (0.880 g, 7.788 mmol) was photolyzed (350 nm) at 10 °C for 195 h. Volatiles were removed in vacuo, and the residue was recrystallized from petroleum ether, yielding 0.309 g of colorless (PMe_3)$_3$Ru($SiEt_3$)H_3 (90% yield). ^{1}H NMR: δ 1.32 (t, J_{HH} = 7.8 Hz, 9H, CH_2CH_3), 1.15 (d, J_{PH} = 5.0 Hz, 27H, PMe_3), 1.07 (q, J_{HH} = 7.8 Hz, 6H, $SiCH_2$), −10.53 (br m, 3H, RuH_3). ^{13}C NMR: δ 26.4 (m, PMe_3), 19.2 (q, $^3J_{PC}$ = 2.9 Hz, $SiCH_2$), 9.8 (s, CH_2CH_3). ^{29}Si NMR: δ 12.7 (q, $^2J_{PSi}$ = 7.7 Hz, *Si*Et$_3$). ^{31}P NMR: δ −5.4 (s, *P*Me$_3$). IR (Nujol): 1899 cm^{-1} (ν_{RuH}). IR (benzene): ν(RuH) = 1897 cm^{-1}. Anal. Calcd for $C_{15}H_{45}P_3Si_1Ru_1$: C, 40.25; H, 10.13. Found: C, 40.53; H, 10.52.

Reaction of *cis*-(PMe_3)$_4$Ru($SiEt_3$)H with H_2. An NMR tube was loaded with a C_6D_6 solution (0.5 mL) of *cis*-(PMe_3)$_4$Ru($SiEt_3$)H (5 mg, 0.001 mmol) and placed under vacuum. Hydrogen (ca. 3 atm) was added, and the tube was sealed. The ^{1}H NMR spectrum was recorded within 5 min and showed complete conversion to (PMe_3)$_3$Ru($SiEt_3$)H_3, with the generation of ca. 1 equiv of free PMe_3.

Reaction of (PMe_3-d_9)(PMe_3)$_3$Ru($SiMe_3$)H with H_2. An NMR tube was loaded with a C_6D_6 solution (0.5 mL) of (PMe_3)$_4$Ru($SiMe_3$)H (9 mg, 0.02 mmol), and the solution was degassed in vacuo. At −196 °C, PMe_3-d_9 (0.35 mmol) was added, and the tube was sealed. Upon thawing, ^{1}H and ^{31}P showed that complete exchange had occurred, forming (PMe_3-d_9)(PMe_3)$_3$Ru($SiMe_3$)H with the labeled phosphine in the position trans to silicon. The tube was opened under inert atmosphere, and the volatiles were removed in vacuo. The solid was dissolved in fresh C_6D_6 (0.5 mL), placed in an NMR tube, and hydrogen (ca. 3 atm) was added. The tube was sealed, and the ^{1}H NMR spectrum was recorded within 5 min. The ^{1}H and ^{31}P NMR spectra showed that the free phosphine was more than 95% PMe_3-d_9 and that the product (PMe_3)$_3$Ru($SiMe_3$)H_3 contained no labeled phosphine.

Photolysis of (PMe_3)$_3$Ru($SiMe_3$)H_3 with PMe_3-d_9. An NMR tube was loaded with a cyclohexane-d_{12} solution (0.4 mL) of (PMe_3)$_3$Ru($SiMe_3$)H_3 (6 mg, 0.015 mol) and C_6Me_6 (2 mg, internal standard).

PMe_3-d_9 (0.179 mmol) was added, and the tube was sealed. The tube was kept at room temperature, and the reaction was monitored by ^{1}H NMR. After 6 days at 25 °C, the ^{1}H NMR spectrum showed that no reaction had occurred. The tube was then photolyzed ($\lambda = 350$ nm) at 10 °C. After 24 h, the ^{1}H NMR spectrum showed that ca. 21% exchange had occurred between the phosphine ligands of $(PMe_3)_3Ru(SiMe_3)H_3$ and the free PMe_3-d_9. After 112.5 h, ca. 52% exchange had occurred.

Reaction of $(PMe_3)_3Ru(SiMe_3)H_3$ in Neat PMe_3-d_9. $(PMe_3)_3Ru(SiMe_3)H_3$ (2 mg, 0.005 mmol) was dissolved in 0.5 mL of PMe_3-d_9 and stirred at 25 °C for 21.5 h in the dark. The mixture was periodically degassed by freeze−pump−thaw cycles to remove any evolved hydrogen. The volatiles were removed in vacuo, and the solids were analyzed by ^{1}H and ^{31}P NMR spectroscopy. The product was composed of ca. 75% of $(PMe_3)_4Ru(SiMe_3)H$ and 25% starting $(PMe_3)_3Ru(SiMe_3)H_3$. Both the ^{1}H and the ^{31}P NMR spectra indicate that the mutually trans PMe_3 positions of $(PMe_3)_4Ru(SiMe_3)H$ do not contain labeled phosphine and that the majority of labeled phosphine (>80%) has been incorporated into the position trans to the silyl group.

Thermolysis of $(PMe_3)_3Ru(SiMe_3)H_3$ and PMe_3 at 70 °C. A NMR tube was loaded with a cyclohexane-d_{12} solution (0.4 mL) of $(PMe_3)_3Ru(SiMe_3)H_3$ (4 mg, 0.01 mmol) and placed under vacuum. PMe_3 (0.02 mmol) was added, and the tube was sealed. The tube was heated at 70 °C, and the reaction was followed by ^{1}H NMR. After 4 h at 70 °C, the ^{1}H NMR spectrum showed ca. 50% conversion to a ca. 10:1 mixture of $(PMe_3)_4RuH_2$ and $(PMe_3)_4Ru(SiMe_3)H$. Free trimethylsilane was also observed. The reaction was complete after 115 h, yielding $(PMe_3)_4RuH_2$ and $HSiMe_3$ as the only products.

Reaction of $(PMe_3)_3Ru(SiMe_3)H_3$ with D_2. An NMR tube was loaded with a C_6D_6 solution (0.5 mL) of $(PMe_3)_3Ru(SiMe_3)H_3$ (20 mg, 0.049 mmol), and the sample was degassed in vacuo. Deuterium (ca. 3 atm) was added, and the tube was sealed. The reaction was monitored by ^{1}H NMR spectroscopy. H_2 was detected after 5 min at 25 °C, and HD was detected after 3 h at 25 °C. The ratio of H_2:HD was ca. 1:1 after 24 h at 25 °C.

Reaction of $(PMe_3)_3Ru(SiEt_3)H_3$ with D_2. An NMR tube was loaded with a C_6D_6 solution (0.5 mL) of $(PMe_3)_3Ru(SiEt_3)H_3$ (20 mg, 0.049 mmol), and the sample was degassed in vacuo. Deuterium (ca. 3 atm) was added, and the tube was sealed. The reaction was monitored by ^{1}H NMR spectroscopy. Only trace amounts of H_2 and HD were detected after 13 days at room temperature.

Exchange Reactions of $(PMe_3)_3Ru(SiR_3)H_3$ with $HSiR_3'$. The general method is described here for the reaction of $(PMe_3)_3Ru(SiMe_3)H_3$ and $HSiMe_2CH_2SiMe_3$: An NMR tube was loaded with a C_6D_6 solution (0.5 mL) of $(PMe_3)_3Ru(SiMe_3)H_3$ (12 mg, 0.03 μmol) and $HSiMe_2CH_2SiMe_3$ (ca. 0.032 mmol) and sealed under vacuum. The reaction was monitored by ^{1}H NMR. Although no reaction was apparent after 0.5 h at 25 °C, a ca. 9:1 ratio of $(PMe_3)_3Ru(SiMe_3)H_3$:$(PMe_3)_3Ru(SiMe_2CH_2SiMe_3)H_3$ was present after 24 h. This ratio did not change at longer reaction times.

Single-Crystal X-ray Diffraction Analyses of $(PMe_3)_4Ru(SiMe_3)Me$ (7a), $(PMe_3)_4Ru(SiMe_3)H$ (1a), and $(PMe_3)_4Ru(SiMe_2CH_2SiMe_3)H$ (1b). X-ray intensity data were collected on a Rigaku R-AXIS IIc area detector employing graphite-monochromated Mo Kα radiation ($\lambda =$ 0.71069 Å). Oscillation images were processed using bioteX,[62] producing a listing of unaveraged F^2 and $\sigma(F^2)$ values which were then passed to the teXsan[63] program package for further processing and structure solution on a Silicon Graphics Indigo R4000 computer.

For $(PMe_3)_4Ru(SiMe_3)Me$, indexing was performed from a series of four 1° oscillations with exposures of 200 s per frame. A hemisphere of data was collected using 8° oscillations with exposures of 200 s per frame and a crystal-to-detector distance of 82 mm. A total of 18 969 reflections were measured over the ranges: $5.02 \le 2\theta \le 50.00°$, $-17 \le h \le 18$, $-12 \le k \le 12$, $-34 \le l \le 36$. The intensity data were corrected for Lorentz and polarization effects but not for absorption. All 4272 unique reflections ($R_{int} = 0.0403$) were used during subsequent structure refinement (200 parameters refined.) The structure was solved by direct methods (SIR92).[64] Refinement was by full-matrix least squares techniques based on F^2 using SHELXL-93.[65] Non-hydrogen atoms were refined anisotropically, and hydrogen atoms were included as constant contributions to the structure factors and were not refined. The maximum Δ/σ in the final cycle of least squares was −0.001, and the two most prominent peaks in the final difference Fourier were +0.504 and −0.583 e/Å^3.

For $(PMe_3)_4Ru(SiMe_2CH_2SiMe_3)H$, indexing was performed from a series of 1° oscillation images with exposures of 100 s per frame. A hemisphere of data was collected using 6° oscillation angles with exposures of 100 s per frame and a crystal-to-detector distance of 82 mm. A total of 28 749 reflections were measured over the ranges $5.16 \le 2\theta \le 54.96°$, $-16 \le h \le 16$, $-30 \le k \le 30$, $-12 \le l \le 13$. The intensity data were corrected for Lorentz and polarization effects but not for absorption. All 6757 unique reflections ($R_{int} = 0.0382$) were used during subsequent structure refinement (292 parameters refined.) The structure was solved by direct methods (SIR92).[64] One of the PMe_3 groups (P3, C7, C8, C9) was found to be rotationally disordered with two contributing rotamers with a ratio of 3:1. Refinement was by full-matrix least squares techniques based on F^2 using SHELXL-93.[65] Non-hydrogen atoms were refined anisotropically, H1 was refined isotropically, and all other hydrogen atoms were refined using a "riding" model. The maximum Δ/σ in the final cycle of least squares was 0.007, and the two most prominent peaks in the final difference Fourier were +0.521 and −0.613 e/Å^3.

For $(PMe_3)_4Ru(SiMe_3)H$, indexing was performed from a series of 1° oscillation images with exposures of 180 s per frame. A hemisphere of data was collected using 3° oscillation angles with exposures of 100 s per frame and a crystal-to-detector distance of 82 mm. A total of 17 931 reflections were measured over the ranges $5.0 \le 2\theta \le 50.7°$, $-18 \le h \le 18$, $-12 \le k \le 12$, $-34 \le l \le 35$. The intensity data were corrected for Lorentz and polarization effects but not for absorption. All 4431 unique reflections ($R_{int} = 0.0267$) were used during subsequent structure refinement (195 parameters refined.) The structure was solved by Patterson methods (DIRDIF94).[66] Refinement was by full-matrix least squares based on F^2 using SHELXL-93.65 The weighting scheme used was $w = 1/[\sigma^2(F_0^2) + 0.0524P^2 + 7.3452P]$, where $P = (F_0^2 + 2F_c^2)/3$. Non-hydrogen atoms were refined anisotropically, and hydrogen atoms were included as constant contributions to the structure factors and were not refined. The maximum Δ/σ in the final cycle of least squares was −0.001, and the two most prominent peaks in the final difference Fourier were +0.458 and −0.539 e/Å^3.

Single-Crystal X-ray Diffraction Analyses of $(PMe_3)_4Ru(SiMe_2H)H$ (1d) and $(PMe_3)_3Ru(SiMe_3)H_3$ (4a). X-ray intensity data were collected on an Enraf-Nonius CAD4 diffractometer employing graphite-monochromated Mo Kα radiation ($\lambda = 0.71073$ Å) and using the ω-2θ scan technique. The cell constants were determined from a least-squares fit of the setting angles for 25 accurately centered reflections. Three standard reflections measured every 3500 s of X-ray exposure showed no intensity decay over the course of data collection.

For $(PMe_3)_4Ru(SiMe_2H)H$, a total of 5945 reflections were measured over the ranges $4.0 \le 2\theta \le 55.0°$, $0 \le h \le 11$, $0 \le k \le 37$, $-12 \le l \le 12$. The intensity data were corrected for Lorentz and polarization effects, and an empirical absorption correction was applied. Of the 5482 unique reflections measured, a total of 3777 reflections ($R_{int} = 0.023$) with $F^2 > 3\sigma(F^2)$ were used during subsequent structure refinement

(62) *bioteX*: *A Suite of Programs for the Collection, Reduction and Interpretation of Imaging Plate Data*; Molecular Structure Corp., 1995.
(63) *teXsan*: *Crystal Structure Analysis Package*; Molecular Structure Corp., 1985 and 1992.
(64) SIR92: Altomare, A.; Burla, M. C.; Camalli, M.; Cascarano, M.; Giocovazzo, C.; Guagliardi, A.; Polidoro, G. *J. Appl. Crystallogr.* **1994**, *27*, 435.
(65) Sheldrick, G. M. *SHELXL-93*: *Program for the Refinement of Crystal Structures*; Göttingen University: Göttingen, Germany, 1993.
(66) Beurskens, P. T.; Admiraal, G.; Beurskens, G.; Bosman, W. P.; de Gelder, R.; Israël, R.; Smits, J. M. M. *The DIRDIF-94 Program System*; Crystallography Laboratory, University of Nijmegen: The Netherlands, 1994.

(189 parameters refined). The structure was solved by standard heavy atom Patterson techniques followed by weighted Fourier syntheses. Hydrogen atoms were found from difference Fourier maps calculated after anisotropic refinement. Refinement was by full-matrix least squares techniques based on F to minimize the quantity $\sum w(|F_o| - |F_c|)^2$ with $w = 1/\sigma^2(F)$. Non-hydrogen atoms were refined anisotropically, the Ru and Si hydrides (H1 and H2) were refined isotropically, and all other hydrogen atoms were included as constant contributions to the structure factors and were not refined. The maximum Δ/σ in the final cycle of least squares was 0.001.

For $(PMe_3)_3Ru(SiMe_3)H_3$, a total of 5658 reflections were measured over the ranges $4 \leq 2\theta \leq 55°$, $0 \leq h \leq 18$, $-12 \leq k \leq 12$, $0 \leq l \leq 21$. The intensity data were corrected for Lorentz and polarization effects, and an empirical absorption correction was applied. Of the 5165 unique reflections measured, a total of 2842 reflections ($R_{int} = 0.023$ with $F^2 > 3\sigma(F^2)$) were used during subsequent structure refinement (166 parameters refined). The structure was solved by standard heavy atom Patterson techniques followed by weighted Fourier syntheses. Hydrogen atoms were found from difference Fourier maps calculated after anisotropic refinement. Refinement was by full-matrix least squares techniques based on F to minimize the quantity $\sum w(|F_o| - |F_c|)^2$ with $w = 1/\sigma^2(F)$. Non-hydrogen atoms were refined anisotropically, the Ru hydrides (H1, H2, and H3) were refined isotropically, and all other hydrogen atoms were included as constant contributions to the structure factors and were not refined. The maximum Δ/σ in the final cycle of least squares was 0.001.

Acknowledgment. We are grateful to the National Science Foundation (CHE-9904798) and Tokyo Electron Massachusetts for support of this work. We also thank Dr. Bernd Mayer for his assistance with the characterization of $(PMe_3)_4Ru(SiMe_2H)H$.

Supporting Information Available: X-ray crystallographic data for **1a**, **1b**, **1d**, **4a**, and **7a** in CIF format. This material is available free of charge via the Internet at http://pubs.acs.org.

JA035131P